Low-energy photon-photon fusion into three pions in generalized chiral perturbation theory

Ll. Ametller,[1] J. Kambor,[2] M. Knecht,[3] and P. Talavera[4]
[1]*Department de Física i Enginyeria Nuclear, UPC, E-08034 Barcelona, Spain*
[2]*Institut für Theoretische Physik, Universität Zürich, CH-8057 Zürich, Switzerland*
[3]*Centre de Physique Théorique, CNRS-Luminy, Case 907, F-13288 Marseille Cedex 9, France*
[4]*Department of Theoretical Physics, University of Lund, Sölvegatan 14A, S-22362 Lund, Sweden*
(Received 27 April 1999; published 24 September 1999)

The processes $\gamma\gamma\to\pi^0\pi^0\pi^0$ and $\gamma\gamma\to\pi^+\pi^-\pi^0$ are considered in generalized chiral perturbation theory, in view of their potential sensitivity to the mechanism of spontaneous breaking of chiral symmetry and to various counterterms. The amplitudes are computed up to order $\mathcal{O}(p^6)$. The event production rates are estimated for the Daphne ϕ-factory and for a future τ-charm factory. [S0556-2821(99)07617-1]

PACS number(s): 12.39.Fe, 11.30.Rd, 13.75.−n, 14.70.Bh

I. INTRODUCTION

In the limit where the masses of the lightest quark flavors u,d, and s are set to zero, the QCD Lagrangian becomes invariant under a chiral $SU(3)_L\times SU(3)_R$ global symmetry. This symmetry is not reproduced by the hadronic spectrum, and must therefore be spontaneously broken towards the diagonal $SU(3)_V$ subgroup. Actually, this spontaneous breaking of chiral symmetry can be shown to follow from very general properties of QCD [1–3]. However, in addition to the existence of eight massless pseudoscalar states coupling to the eight conserved axial vector currents, nothing is known from ''first principles'' about the actual mechanism of spontaneous breaking of chiral symmetry. The widespread belief in that matter is that it proceeds through the formation of a strong quark-antiquark condensate, $\langle\bar{q}q\rangle\sim-(250\,\mathrm{MeV})^3$, where $\langle\bar{q}q\rangle$ denotes the single flavor quark-antiquark condensate in the $SU(2)$ chiral limit:

$$\langle\bar{q}q\rangle=\langle\bar{u}u\rangle|_{m_u=m_d=0}=\langle\bar{d}d\rangle|_{m_u=m_d=0}. \tag{1.1}$$

In particular, this means that once the light quark masses m_u, m_d, and m_s are turned on, the mass of the pion is assumed to be dominated by the contribution linear in quark masses [4],

$$-\frac{2\hat{m}\langle\bar{q}q\rangle}{F^2M_\pi^2}\sim 1,\quad \hat{m}=\frac{m_u+m_d}{2}, \tag{1.2}$$

where F stands for the pion decay constant F_π (the normalization we use corresponds to the numerical value $F_\pi=92.4\,\mathrm{MeV}$ [5]) in the same two-flavor chiral limit,

$$F=F_\pi|_{m_u=m_d=0}. \tag{1.3}$$

However, our present theoretical knowledge of nonperturbative aspects in QCD does not exclude a picture where the condensate would be much smaller, say, $\langle\bar{q}q\rangle\sim-(100\,\mathrm{MeV})^3$, or even vanishing. How the latter possibility may arise in QCD has been discussed recently [6,7] in terms of spectral properties of the Dirac operator. On the other hand, it has also been suggested [8] that a strictly vanishing condensate in the chiral limit could be excluded by an inequality [9] between the correlator $\langle A_\mu(x)A^\mu(0)\rangle$ of two axial currents and the two-point function $\langle P(x)P(0)\rangle$ of the pseudoscalar quark bilinear density $P(x)\equiv(\bar{q}i\gamma_5 q)(x)$. This inequality, however, has only been established so far for bare quantities, i.e., in the presence of an ultraviolet cutoff Λ_{UV}. As the cutoff is removed, the pseudoscalar density $P(x)$ needs to be renormalized, whereas the (partially) conserved axial vector current $A_\mu(x)$ remains unaffected. Strictly speaking, the claim of Ref. [8] is that $\langle\bar{q}q\rangle(\Lambda_{\mathrm{UV}})\neq 0$ for finite Λ_{UV}, which does not, *a priori*, exclude the possibility of a vanishing condensate in the limit $\Lambda_{\mathrm{UV}}\to\infty$ [6]. Finally, Ref. [10] provides an example of a different approach which, within a variational framework, leads to a nonvanishing, but nevertheless small, value of $\langle\bar{q}q\rangle$.

Clearly, in order to settle the question of the mechanism of spontaneous chiral symmetry breaking on a purely theoretical level, a major breakthrough in our understanding of nonperturbative aspects of confining gauge theories is required. Instead, one may try a phenomenological approach, and look for experimental observables which could provide the relevant information. In this respect, low-energy π-π scattering in the S wave has been put forward as a process particularly sensitive to the size of the condensate [11,12] (for recent discussions, see, e.g., [13,7]). This can be most conveniently seen in the framework of the effective Lagrangian [14–16]. In order to incorporate the possibility of a small condensate, the usual counting has however to be modified. As explained in Refs. [11,17], a consistent expansion scheme, usually referred to as generalized chiral perturbation theory (GChPT), is obtained by taking (from now on, we restrict ourselves to the case of two massless flavors only)

$$m_u,m_d\sim\mathcal{O}(p),\quad B\sim\mathcal{O}(p), \tag{1.4}$$

with p being a generic momentum, much smaller than the typical hadronic scale $\Lambda_H\sim 1\,\mathrm{GeV}$, and

$$B\equiv-\frac{\langle\bar{q}q\rangle}{F^2}. \tag{1.5}$$

With this counting, the effective Lagrangian at lowest order, which consists of all chiral invariant terms of order $\mathcal{O}(p^2)$, reads [11]

$$\tilde{\mathcal{L}}^{(2)}=\frac{1}{4}F^2\{\langle D_\mu U^+ D^\mu U\rangle+2B\langle U^+\chi+\chi^+U\rangle+A\langle(U^+\chi)^2 +(\chi^+U)^2\rangle+Z^P\langle U^+\chi-\chi^+U\rangle^2+h_0\langle\chi^+\chi\rangle +h_1(\det\chi+\det\chi^+)\}. \tag{1.6}$$

The matrix U collects the pion fields (throughout, we adopt the Condon and Shortley phase convention),

$$U=e^{i\phi/F},\quad \phi=\begin{pmatrix}\pi^0 & -\sqrt{2}\pi^+\\ \sqrt{2}\pi^- & -\pi^0\end{pmatrix}. \tag{1.7}$$

The notation is as in Refs. [15,16], except that χ, the quantity that contains the scalar and pseudoscalar sources, is defined without the usual factor $2B$,

$$\chi=s+ip=\mathcal{M}+\cdots,\quad \mathcal{M}=\mathrm{diag}(m_u,m_d). \tag{1.8}$$

The covariant derivative contains the external vector and axial sources,

$$D_\mu U=\partial_\mu U-i[v_\mu,U]-i\{a_\mu,U\}. \tag{1.9}$$

This is to be contrasted with standard chiral perturbation theory (SChPT) [15,16], which assumes a large condensate, and hence the counting rule $m_u,m_d\sim\mathcal{O}(p^2)$, $B\sim\Lambda_H$, so that only the first two terms on the right-hand side of Eq. (1.6) are taken into account at leading order. It easily follows from Eq. (1.6) that the lowest order expression of the pion mass is now given as by[1]

$$M_\pi^2=2\hat{m}B+4\hat{m}^2A+\cdots, \tag{1.10}$$

where the ellipsis stands for higher order corrections. At the same level of approximation in the chiral expansion, the π-π scattering amplitude can be written as [11]

$$A(s|t,u)=\beta\frac{\left(s-\frac{4}{3}M_\pi^2\right)}{F^2}+\alpha\frac{M_\pi^2}{3F^2}+\cdots, \tag{1.11}$$

with $\beta=1+\mathcal{O}(\hat{m})$, while at this order the parameter α is directly related to the $\langle\bar{q}q\rangle$ condensate through

$$\alpha=4-3\left(\frac{2\hat{m}B}{M_\pi^2}\right)+\mathcal{O}(\hat{m}). \tag{1.12}$$

The case (1.2) of a strong condensate corresponds to $\alpha=1$, whereas the extreme limit where the condensate would vanish yields $\alpha=4$. Notice that the above expression for $A(s|t,u)$ is not affected by the additional terms in Eq. (1.6) and reproduces the result first obtained by Weinberg [18], $A(s|t,u)=(s-2\hat{m}B)/F^2+\cdots$. The difference between the standard case and deviations from it lies here only in the leading-order expression (1.10) of the pion mass and its relation to the condensate. Higher orders in the chiral expansion will modify the simple expression (1.11), but the correlation between low-energy π-π scattering and the value of the ratio $2\hat{m}B/M_\pi^2$ subsists, and can be studied in a controlled way within the generalized chiral expansion [12]. Available data on low-energy π-π phases, which are dominated by the Geneva–Saclay K_{l4} experiment [19], do, however, not possess the required accuracy in order to distinguish between the different alternatives at present. Forthcoming experiments, such as new K_{l4} experiments, conducted by the BNL865 Collaboration [20] or planed at the Daphne ϕ-factory [21], and the DIRAC experiment at CERN [22], represent promising prospects in this direction.

In order to create a (hopefully convergent) set of evidence *pro* or *contra* a specific picture of spontaneous breaking of chiral symmetry, it remains however important to explore other possibilities, and to find other processes which, at the theoretical level, can be shown to exhibit a reasonably strong dependence on the value of the condensate. The present work was motivated by the above consideration and the following observation. A straightforward reanalysis in GChPT of the existing SChPT calculations [23–25] at lowest order shows that the two amplitudes for the production of three pions in low-energy photon-photon collisions involve the parameter α already at tree level. In the case of $\gamma\gamma\to\pi^0\pi^0\pi^0$, the amplitude reads

$$\mathcal{A}^N=\frac{e^2}{4\pi^2F_\pi^3}\epsilon^{\mu\nu\alpha\beta}k_\mu\epsilon_\nu k'_\alpha\epsilon'_\beta\frac{\alpha M_\pi^2}{s-M_\pi^2}+\cdots, \tag{1.13}$$

while for $\gamma\gamma\to\pi^+\pi^-\pi^0$ we find

$$\mathcal{A}^C=\frac{e^2}{4\pi^2F_\pi^3}\epsilon_{\mu\nu\alpha\beta}k^\mu\epsilon^\nu k'^\alpha\epsilon'^\beta \times\left(1-\frac{(p_++p_-)^2-M_\pi^2+\frac{1}{3}(\alpha-1)M_\pi^2}{s-M_\pi^2}\right) +\frac{e^2}{4\pi^2F_\pi^3}\epsilon_{\mu\nu\alpha\beta}k'^\mu\epsilon'^\nu p_0^\alpha\left(-\epsilon^\beta+\frac{\epsilon\cdot p_-}{k\cdot p_-}p_+^\beta +\frac{\epsilon\cdot p_+}{k\cdot p_+}p_-^\beta\right)+\frac{e^2}{4\pi^2F_\pi^3}\epsilon_{\mu\nu\alpha\beta}k^\mu\epsilon^\nu p_0^\alpha \times\left(-\epsilon'^\beta+\frac{\epsilon'\cdot p_-}{k'\cdot p_-}p_+^\beta+\frac{\epsilon'\cdot p_+}{k'\cdot p_+}p_-^\beta\right)+\cdots. \tag{1.14}$$

In these expressions, k and k' (ϵ and ϵ') denote the momenta (polarizations) of the two photons, while p_+, p_- and p_0 are the pion momenta. The ellipses stand for higher order corrections which will be considered later. Diagrammati-

[1]We neglect the mass difference m_u-m_d and set $m_u=m_d=\hat{m}$.

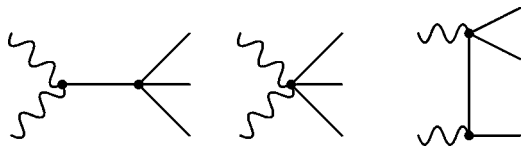

FIG. 1. The lowest order contributions to the $\gamma\gamma\to\pi\pi\pi$ amplitudes. The α dependence in $\mathcal{A}^N$ and $\mathcal{A}^C$ comes from the vertex for (virtual) π-π scattering in the first graph, which is the only one to contribute in the case of the neutral amplitude.

cally, the origin of the dependence on α lies in the presence of one-pion reducible contributions to the two amplitudes, see Fig. 1.

Therefore, the leading-order neutral amplitude $\mathcal{A}^N$ increases as the condensate decreases. For a strictly vanishing condensate ($\alpha=4$), the cross section at low energies is thus enhanced by a factor 16 as compared to the standard case of a strong condensate ($\alpha=1$)! In the charged case, the situation is less favorable. At threshold, the average over the photon polarizations of the modulus squared of the amplitude is still proportional to the square of α,

$$\frac{1}{4}\sum_{\text{pol}}|\mathcal{A}^C|^2_{\text{thr}}=\frac{1}{4}\left(\frac{e^2}{4\pi^2F_\pi^3}\right)^2\frac{9M_\pi^4}{128}\alpha^2, \tag{1.15}$$

but the sensitivity on α of the corresponding total *cross section* $\sigma^C(s,\alpha)$ rapidly decreases with increasing energy. For instance, the ratio $\sigma^C(s,\alpha=3)/\sigma^C(s,\alpha=1)$ is equal to 4.48 at $\sqrt{s}=450$ MeV, i.e., just above threshold, but drops to 1.68 at $\sqrt{s}=500$ MeV and becomes less than 1.10 at $\sqrt{s}\gtrsim 600$ MeV. For the case $\alpha=2$, the corresponding ratio is equal to 2.21 at $\sqrt{s}=450$ MeV, but the effect is less than 25% at $\sqrt{s}=500$ MeV, while it barely reaches a few percent at $\sqrt{s}\gtrsim 600$. Thus, the interference between the two kinematical structures contributing to the amplitude $\mathcal{A}^C$, which is responsible, at low energies, for the suppression of the cross section in the charged channel as compared to the cross section in the neutral channel [25], also washes out the dependence on the value of the $\langle\bar{q}q\rangle$ condensate as soon as one leaves the threshold region. Considering definite polarization configurations for the two photons does not improve the situation: For parallel polarizations of the two photons, the part of $\mathcal{A}^C$ which is sensitive to α does not contribute to the cross section, whereas for polarizations taken along orthogonal axes, the same interference effect is again fully at work. Furthermore, both cross sections rapidly rise above threshold, so that the effect of higher orders also needs to be investigated. The purpose of this paper is precisely to investigate these higher order effects at the one-loop level in GChPT. In fact, at next-to-leading order new tensorial structures appear both in the neutral and in the charged amplitude [25,26], whereas the pion loops provide additional sources of dependence with respect to α, so that their behavior with respect to changes in the value of the condensate could be modified to some extent.

Accordingly, the rest of the paper is organized as follows: The general kinematical structure of the two amplitudes $\mathcal{A}^N$ and $\mathcal{A}^C$, as well as their properties under isospin symmetry, are the subject of Sec. II. The construction of the effective lagrangian of GChPT at one-loop order in the two-flavor case is briefly discussed in Sec. III. Section IV is devoted to the actual calculation of the two amplitudes to one-loop precision. The counterterms which are involved in these expressions and several numerical results are discussed in Sec. V. A summary and conclusion are presented in Sec. VI. Additional material concerning the structure and the renormalization at one-loop order of the effective Lagrangian of GChPT is presented in Appendix A, and details on the evaluation of some counterterms have been gathered in Appendix B.

II. KINEMATICS AND ISOSPIN SYMMETRY

The amplitudes $\mathcal{A}^N$ and $\mathcal{A}^C$ for the processes

$$\begin{aligned}\gamma(k)\,\gamma(k')&\to\pi^0(p_1)\,\pi^0(p_2)\,\pi^0(p_3),\\ \gamma(k)\,\gamma(k')&\to\pi^+(p_+)\,\pi^-(p_-)\,\pi^0(p_0),\end{aligned} \tag{2.1}$$

are obtained from the matrix elements

$$\begin{aligned}\langle\pi^0(p_1)\,\pi^0(p_2)\,\pi^0(p_3)\ \text{out}|\,\gamma(k,\epsilon)\,\gamma(k',\epsilon')\ \text{in}\rangle&=i(2\pi)^4\delta^4(P_f-P_i)\mathcal{A}^N,\\ \langle\pi^+(p_+)\,\pi^-(p_-)\,\pi^0(p_0)\ \text{out}|\,\gamma(k,\epsilon)\,\gamma(k',\epsilon')\ \text{in}\rangle&=i(2\pi)^4\delta^4(P_f-P_i)\mathcal{A}^C,\end{aligned} \tag{2.2}$$

respectively, with

$$\begin{aligned}\mathcal{A}^N(k,\epsilon;k',\epsilon';p_1,p_2,p_3)&=ie^2\epsilon_\mu(k)\epsilon'_\nu(k')\int d^4x e^{-ik\cdot x}\langle\pi^0(p_1)\,\pi^0(p_2)\,\pi^0(p_3)\ \text{out}|T\{j^\mu(x)j^\nu(0)\}|\Omega\rangle,\\ \mathcal{A}^C(k,\epsilon;k',\epsilon';p_0,p_+,p_-)&=ie^2\epsilon_\mu(k)\epsilon'_\nu(k')\int d^4x e^{-ik\cdot x}\langle\pi^+(p_+)\,\pi^-(p_-)\,\pi^0(p_0)\ \text{out}|T\{j^\mu(x)j^\nu(0)\}|\Omega\rangle.\end{aligned} \tag{2.3}$$

In the above expressions, $j_\mu(x)$ denotes the electromagnetic current, with its usual decomposition into an isotriplet and an isosinglet component, $j_\mu = j_\mu^3 + j_\mu^0$, while $|\Omega\rangle$ stands for the QCD vacuum with massive light quarks, but in the absence of electromagnetism (radiative corrections to the two processes (2.1) are not considered here). Since we also neglect isospin breaking effects due to $m_u \neq m_d$, Bose symmetry and G parity constrain the three final pions to be in an $I=1$ total isospin state. Thus the matrix elements in Eq. (2.3) only involve the $I=1$ component of the product of the two electromagnetic currents,

$$T\{j_\mu(x) j_\nu(0)\}_{I=1} = T\{j_\mu^3(x) j_\nu^0(0) + j_\mu^0(x) j_\nu^3(0)\}. \tag{2.4}$$

Therefore, isospin invariance relates the two amplitudes $\mathcal{A}^C$ and $\mathcal{A}^N$ in a simple way. With the Condon and Shortley phase convention adopted in Eq. (1.7), this relation reads

$$-\mathcal{A}^N(k,\epsilon;k',\epsilon';p_1,p_2,p_3) = \mathcal{A}^C(k,\epsilon;k',\epsilon';p_1,p_2,p_3) + \text{cyclic}\,(p_1,p_2,p_3), \tag{2.5}$$

where ''cyclic (p_1,p_2,p_3)'' indicates that the contributions arising from cyclic permutations over the pion momenta p_1, p_2, and p_3 have to be added.

Up to permutations of the momenta and polarizations of the photons, and/or permutations of the momenta of the charged pions, the amplitude $\mathcal{A}^C$ may be decomposed into six independent Lorentz invariant amplitudes

$$\begin{aligned}
\mathcal{A}^C(k,\epsilon;k',\epsilon';p_0,p_+,p_-) &= \mathcal{A}_1^C(k,k';p_0,p_+,p_-)\, t_1(k,\epsilon;k',\epsilon') \\
&+ \sum_{i=2,3} \left[\mathcal{A}_i^C(k,k';p_0,p_+,p_-)\, t_i(k,\epsilon;k',\epsilon';p_0,p_+,p_-) + \begin{pmatrix} k \\ \epsilon \end{pmatrix} \leftrightarrow \begin{pmatrix} k' \\ \epsilon' \end{pmatrix} \right] \\
&+ \sum_{i=4,5,6} \left\{ \left[\mathcal{A}_i^C(k,k';p_0,p_+,p_-)\, t_i(k,\epsilon;k',\epsilon';p_0,p_+,p_-) + \begin{pmatrix} k \\ \epsilon \end{pmatrix} \leftrightarrow \begin{pmatrix} k' \\ \epsilon' \end{pmatrix} \right] + [p_+ \leftrightarrow p_-] \right\},
\end{aligned} \tag{2.6}$$

with $(p_{ij} \equiv p_i + p_j,\ i,j = +,-,0)$

$$\begin{aligned}
t_1(k,\epsilon;k',\epsilon') &= \epsilon_{\mu\nu\alpha\beta} k^\mu \epsilon^\nu k'^\alpha \epsilon'^\beta, \\
t_2(k,\epsilon;k',\epsilon';p_0,p_+,p_-) &= \epsilon_{\mu\nu\alpha\beta} k'^\mu \epsilon'^\nu p_0^\alpha \left(-\epsilon^\beta + \frac{\epsilon\cdot p_-}{k\cdot p_-} p_+^\beta + \frac{\epsilon\cdot p_+}{k\cdot p_+} p_-^\beta \right), \\
t_3(k,\epsilon;k',\epsilon';p_0,p_+,p_-) &= \epsilon_{\mu\nu\alpha\beta} \left(-\epsilon^\mu + \frac{\epsilon\cdot p_{+-}}{k\cdot p_{+-}} k^\mu \right) k'^\nu p_0^\alpha \epsilon'^\beta, \\
t_4(k,\epsilon;k',\epsilon';p_0,p_+,p_-) &= \epsilon_{\mu\nu\alpha\beta} \left(-\epsilon^\mu + \frac{\epsilon\cdot p_{+0}}{k\cdot p_{+0}} k^\mu \right) k'^\nu p_-^\alpha \epsilon'^\beta, \\
t_5(k,\epsilon;k',\epsilon';p_0,p_+,p_-) &= \epsilon_{\mu\nu\alpha\beta} k'^\mu p_+^\nu p_-^\alpha \epsilon'^\beta \left(\frac{\epsilon\cdot p_{+0}}{k\cdot p_{+0}} - \frac{\epsilon\cdot p_+}{k\cdot p_+} \right), \\
t_6(k,\epsilon;k',\epsilon';p_0,p_+,p_-) &= \epsilon_{\mu\nu\alpha\beta} \left(-\epsilon^\mu + \frac{\epsilon\cdot p_+}{k\cdot p_+} k^\mu \right) k'^\nu p_-^\alpha \epsilon'^\beta.
\end{aligned} \tag{2.7}$$

In the following, we shall compute the amplitudes $\mathcal{A}^C$ and $\mathcal{A}^N$ within the framework of generalized chiral perturbation theory up to the order of one-loop. At this level of accuracy of the chiral expansion, the amplitude $\mathcal{A}^N$ does not yet receive its full structure as implied by Eqs. (2.6) and (2.5); rather, it takes the simpler form $(p_{ij} \equiv p_i + p_j,\ i,j = 1,2,3)$

$$\begin{aligned}
\mathcal{A}^N(k,\epsilon;k'\epsilon';p_1,p_2,p_3) &= \mathcal{A}_1^N(k,k';p_1,p_2,p_3)\, t_1(k,\epsilon;k',\epsilon') \\
&+ \left[\mathcal{A}_2^N(k,k';p_1,p_2,p_3)\, \epsilon_{\mu\nu\alpha\beta} \left(\epsilon'^\mu - \frac{\epsilon'\cdot p_{12}}{k'\cdot p_{12}} k'^\mu \right) p_{12}^\nu \epsilon^\alpha k^\beta + \text{cyclic}(p_1,p_2,p_3) \right] \\
&+ \left[\begin{pmatrix} k \\ \epsilon \end{pmatrix} \leftrightarrow \begin{pmatrix} k' \\ \epsilon' \end{pmatrix} \right] + \cdots,
\end{aligned} \tag{2.8}$$

where the ellipsis stands for higher order terms in the chiral expansion. In order that Eq. (2.8) follows from Eqs. (2.5) and (2.6), it is *sufficient* that the one-loop charged amplitudes $\mathcal{A}_i^C$ satisfy the following conditions: (i) $\mathcal{A}_2^C(k,k';p_0,p_+,p_-)$

$-\mathcal{A}_5^C(k,k';p_+,p_-,p_0)$ is entirely symmetric under permutations of the pion momenta p_+,p_-,p_0; (ii) $k\cdot p_0[\mathcal{A}_5^C(k,k';p_0,p_+,p_-)+\mathcal{A}_6^C(k,k';p_0,p_+,p_-)]=k\cdot p_+[\mathcal{A}_5^C(k,k';p_+,p_0,p_-)+\mathcal{A}_6^C(k,k';p_+,p_0,p_-)]$; (iii) $\mathcal{A}_5^C(k,k';p_0,p_+,p_-)=\mathcal{A}_5^C(k,k';p_+,p_0,p_-)$. Furthermore, the two neutral amplitudes have then the following expressions in terms of the charged ones:

$$\mathcal{A}_1^N(k,k';p_1,p_2,p_3)=-\mathcal{A}_1^C(k,k';p_1,p_2,p_3)+\left[\frac{1}{3}\mathcal{A}_2^C(k,k';p_1,p_2,p_3)+\mathcal{A}_3^C(k,k';p_3,p_1,p_2)+\mathcal{A}_4^C(k,k';p_1,p_2,p_3)\right.$$
$$\left.+\mathcal{A}_4^C(k,k';p_2,p_1,p_3)+\mathcal{A}_6^C(k,k';p_1,p_2,p_3)+\mathcal{A}_6^C(k,k';p_2,p_1,p_3)+\frac{2}{3}\mathcal{A}_5^C(k,k';p_2,p_3,p_1)\right]$$
$$+\left[\begin{pmatrix}k\\ \epsilon\end{pmatrix}\leftrightarrow\begin{pmatrix}k'\\ \epsilon'\end{pmatrix}\right]+\text{cyclic}(p_1,p_2,p_3), \tag{2.9}$$

and

$$-\mathcal{A}_2^N(k,k';p_1,p_2,p_3)=[\mathcal{A}_4^C(k,k';p_1,p_2,p_3)+\mathcal{A}_6^C(k,k';p_1,p_2,p_3)]+[p_1\leftrightarrow p_2]+\mathcal{A}_3^C(k,k';p_1,p_2,p_3)+\mathcal{A}_5^C(k,k';p_2,p_1,p_3). \tag{2.10}$$

III. THE EFFECTIVE LAGRANGIAN IN GChPT

Before proceeding with the calculation of the amplitudes $\mathcal{A}^C$ and $\mathcal{A}^N$ in the next section, we first discuss the main features of the structure of the low-energy generating functional in the case of two light flavors that we need for our subsequent calculation. Additional details and results otherwise not available from the existing literature are presented in Appendix A for the convenience of the interested reader.

The structure of the effective Lagrangian $\mathcal{L}^{\text{eff}}$ is independent of the underlying mechanism of spontaneous chiral symmetry breaking. It consists of an infinite tower of chiral invariant contributions

$$\mathcal{L}^{\text{eff}}=\sum_{(k,l)}\mathcal{L}_{(k,l)}, \tag{3.1}$$

where $\mathcal{L}_{(k,l)}$ contains k powers of covariant derivatives and l powers of the scalar or pseudoscalar sources. In the chiral limit, these terms behave as

$$\mathcal{L}_{(k,l)}\sim\left(\frac{p}{\Lambda_H}\right)^k\left(\frac{m_{\text{quark}}}{\Lambda_H}\right)^l, \tag{3.2}$$

with $m_{\text{quark}}=m_u,m_d$, and p stands for a typical external momentum. The standard approach not only assumes $m_{\text{quark}}\ll\Lambda_H$, but also $m_{\text{quark}}\ll B/2A$, such as to enforce the dominance of the term linear in m_{quark} in the expression of the pion mass (1.10). This allows us to reorganize the double expansion (3.1) as [15,16]

$$\mathcal{L}^{\text{eff}}=\mathcal{L}^{(2)}+\mathcal{L}^{(4)}+\mathcal{L}^{(6)}+\cdots, \tag{3.3}$$

where $\mathcal{L}^{(d)}=\Sigma\mathcal{L}_{(k,l)}$ with $k+2l=d$. The generalized framework considers the possibility that the condensate could be much smaller than usually believed, so that for the actual values of the quark masses one could have $m_{\text{quark}}\sim B/2A$ and still $m_{\text{quark}}\ll\Lambda_H$. This leads to a different reorganization of the double expansion (3.1), namely,

$$\mathcal{L}^{\text{eff}}=\tilde{\mathcal{L}}^{(2)}+\tilde{\mathcal{L}}^{(3)}+\tilde{\mathcal{L}}^{(4)}+\tilde{\mathcal{L}}^{(5)}+\tilde{\mathcal{L}}^{(6)}+\cdots, \tag{3.4}$$

where now, according to Eq. (1.4), $\tilde{\mathcal{L}}^{(d)}=\Sigma B^n\mathcal{L}_{(k,l)}$ with $k+l+n=d$ [11,17].

The leading order of the generalized expansion is described by $\tilde{\mathcal{L}}^{(2)}$, which in the two flavor case was given in Sec. I, Eq. (1.6). For our purposes, we need only to consider the situation without an axial source, and with the vector source restricted to the (classical) photon field A_μ,

$$a_\mu=0,\quad v_\mu=eA_\mu Q, \tag{3.5}$$

where Q stands for the charge matrix of the two light quark flavors u and d,

$$Q=\begin{pmatrix}\frac{2}{3} & 0\\ 0 & -\frac{1}{3}\end{pmatrix}. \tag{3.6}$$

In GChPT, the next-to-leading order corrections are of order $\mathcal{O}(p^3)$, and still occur before the loop corrections. They are embodied in $\tilde{\mathcal{L}}^{(3)}=\mathcal{L}_{(2,1)}+\mathcal{L}_{(0,3)}$, which reads[2]

$$\tilde{\mathcal{L}}^{(3)}=\frac{1}{4}F^2\{\xi^{(2)}\langle D_\mu U^+D^\mu U(\chi^+U+U^+\chi)\rangle+\rho_1^{(2)}\langle(\chi^+U)^3+(U^+\chi)^3\rangle+\rho_2^{(2)}\langle(\chi^+U+U^+\chi)\chi^+\chi\rangle$$
$$+\rho_3^{(2)}\langle\chi^+U-U^+\chi\rangle\langle(\chi^+U)^2-(U^+\chi)^2\rangle+\rho_4^{(2)}\langle(\chi^+U)^2+(U^+\chi)^2\rangle\langle\chi^+U+U^+\chi\rangle$$

[2]The superscript (2) is meant to distinguish the low energy constants $\xi^{(2)}$, $\rho_i^{(2)}$ from the similar ones that occur in the expression of $\tilde{\mathcal{L}}^{(3)}$ in the three flavor case [11,17].

$$+\rho_5^{(2)}\langle\chi^+\chi\rangle\langle\chi^+U+U^+\chi\rangle\}. \tag{3.7}$$

From order $\mathcal{O}(p^4)$ onward, the contributions to $\mathcal{L}^{\rm eff}$ come with either even or odd intrinsic parity, $\tilde{\mathcal{L}}^{(d)}=\tilde{\mathcal{L}}^{(d)}_+ + \tilde{\mathcal{L}}^{(d)}_-$ for $d\geqslant 4$, or $\mathcal{L}_{(k,l)}=\mathcal{L}^+_{(k,l)}+\mathcal{L}^-_{(k,l)}$ for $k\geqslant 4$. The tree-level contributions at order $\mathcal{O}(p^4)$ in the *even intrinsic parity sector* are contained in

$$\tilde{\mathcal{L}}^{(4)}_+=\mathcal{L}^+_{(4,0)}+\mathcal{L}_{(2,2)}+\mathcal{L}_{(0,4)}+B^2\mathcal{L}'_{(0,2)}+B\mathcal{L}'_{(2,1)}+B\mathcal{L}'_{(0,3)}. \tag{3.8}$$

The part without explicit chiral symmetry breaking $\mathcal{L}^+_{(4,0)}$ is described by the same low-energy constants l_1, l_2, l_5, l_6, and h_2 as in the standard case [15],

$$\begin{aligned}\mathcal{L}^+_{(4,0)}=&\frac{l_1}{4}\langle D^\mu U^+ D_\mu U\rangle^2+\frac{l_2}{4}\langle D^\mu U^+ D^\nu U\rangle\langle D_\mu U^+ D_\nu U\rangle\\&+l_5\langle F^{\rm L}_{\mu\nu}UF^{{\rm L}\mu\nu}U^+\rangle+\frac{il_6}{2}\langle F^{\rm R}_{\mu\nu}d^\mu U d^\nu U^+\\&+F^{\rm L}_{\mu\nu}d^\mu U^+ d^\nu U\rangle-\Big(2h_2+\tfrac{1}{2}l_5\Big)\langle F^{\rm R}_{\mu\nu}F^{{\rm R}\mu\nu}\\&+F^{\rm L}_{\mu\nu}F^{{\rm L}\mu\nu}\rangle.\end{aligned} \tag{3.9}$$

The contributions $\mathcal{L}_{(2,2)}$ and $\mathcal{L}_{(0,4)}$ associated to quark mass corrections are displayed in Appendix A. Notice that in the standard framework the contributions from $\mathcal{L}_{(2,2)}$ and from $\mathcal{L}_{(0,4)}$ would count as order $\mathcal{O}(p^6)$ and order $\mathcal{O}(p^8)$, respectively.[3]

Next, we turn to the *odd intrinsic parity sector*. There, the first contribution starts at order $\mathcal{O}(p^4)$, and since it is entirely fixed by the short distance properties of QCD, there is no difference between the standard and the generalized case, $\mathcal{L}^{(4)}_-=\tilde{\mathcal{L}}^{(4)}_-=\mathcal{L}^-_{(4,0)}$. In the two flavor case, $\mathcal{L}^-_{(4,0)}$ vanishes in the absence of external sources. In the presence of an electromagnetic field, it reads

$$\begin{aligned}\mathcal{L}^-_{(4,0)}=&\frac{e}{16\pi^2}\epsilon^{\mu\nu\alpha\beta}A_\mu\langle Q(\partial_\nu U\partial_\alpha U^+\partial_\beta U U^+\\&-\partial_\nu U^+\partial_\alpha U\partial_\beta U^+ U)\rangle\\&-\frac{ie^2}{8\pi^2}\epsilon^{\mu\nu\alpha\beta}\partial_\mu A_\nu A_\alpha\Big\langle Q^2\partial_\beta U U^+ + Q^2 U^+\partial_\beta U\\&-\tfrac{1}{2}QUQ\partial_\beta U^+ + \tfrac{1}{2}QU^+Q\partial_\beta U\Big\rangle.\end{aligned} \tag{3.10}$$

The computation of the amplitudes $\mathcal{A}^N$ and $\mathcal{A}^C$ to one loop also involves the counterterms from $\tilde{\mathcal{L}}^{(5)}_-=\mathcal{L}^-_{(4,1)}$ and from $\tilde{\mathcal{L}}^{(6)}_-=\mathcal{L}^-_{(6,0)}+\mathcal{L}^-_{(4,2)}$. In the standard case, both $\mathcal{L}^-_{(4,1)}$ and $\mathcal{L}^-_{(6,0)}$ count as order $\mathcal{O}(p^6)$, and have been discussed before in the literature[4] [30,31,27]. Borrowing from the last and most recent of these references, we obtain

$$\begin{aligned}\mathcal{L}^-_{(4,1)}=&\frac{1}{4\pi^2}\epsilon_{\mu\nu\alpha\beta}\{iA_4\langle[\chi]_-[G^{\mu\nu}]_+[G^{\alpha\beta}]_+\rangle+iA_6\langle[\chi]_-\rangle\\&\times\langle[G^{\mu\nu}]_+[G^{\alpha\beta}]_+\rangle\\&+A_{12}\langle[D^\mu U]_-[D^\nu U]_-([\chi]_-[G^{\alpha\beta}]_+\\&+[G^{\alpha\beta}]_+[\chi]_-)\rangle\\&+A_{13}\langle[D^\mu U]_-[\chi]_-[D^\nu U]_-[G^{\alpha\beta}]_+\rangle\cdots\},\end{aligned} \tag{3.11}$$

and

$$\begin{aligned}\mathcal{L}^-_{(6,0)}=&\frac{1}{4\pi^2}\epsilon_{\mu\nu\alpha\beta}\{iA_2\langle[D^\mu U]_-([D^\nu G^{\gamma\alpha}]_+[G^\beta_\gamma]_+\\&-[G^{\gamma\alpha}]_+[D^\nu G^\beta_\gamma]_+)\rangle\\&+iA_3\langle[D^\mu U]_-([D_\gamma G^{\gamma\nu}]_+[G^{\alpha\beta}]_+\\&-[G^{\gamma\nu}]_+[D_\gamma G^{\alpha\beta}]_+-[D_\gamma G^{\alpha\beta}]_+[G^{\gamma\nu}]_+\\&+[G^{\alpha\beta}]_+[D_\gamma G^{\gamma\nu}]_+)\rangle\\&+A_7\langle[D^\alpha D^\gamma U]_-([D_\gamma U]_-[D^\beta U]_-[G^{\mu\nu}]_+\\&-[G^{\mu\nu}]_+[D^\beta U]_-[D_\gamma U]_-)\rangle\\&+A_8\langle[D^\alpha D^\gamma U]_-([D^\beta U]_-[D_\gamma U]_-[G^{\mu\nu}]_+\\&-[G^{\mu\nu}]_+[D_\gamma U]_-[D^\beta U]_-)\rangle+\cdots\}.\end{aligned} \tag{3.12}$$

Here, we have only listed those terms that will actually contribute to the processes under study, when the mass-shell conditions for the momenta and polarizations of the photons are taken into account. We have however kept the numbering of the low-energy constants introduced in [27], but we have, for convenience, changed their normalization by an overall factor $1/4\pi^2$. The notation is otherwise as in [27], except for the fact that the source χ does not contain the factor $2B$, see Eq. (1.8).

The last piece we need for a full one-loop computation of the amplitudes (2.3) is $\mathcal{L}^-_{(4,2)}$. It counts as order $\mathcal{O}(p^8)$ in the *standard* case, and is not available from the existing literature. These contributions, which are order $\mathcal{O}(\hat{m}^2)$ corrections to $\mathcal{L}^-_{(4,0)}$, are expected to be small in the two-flavor chiral expansion, and will be parametrized appropriately in the one-loop expressions of the amplitudes $\mathcal{A}^C$ and $\mathcal{A}^N$ given in the next section. The determination of the combinations of low-energy constants that enter these amplitudes will be discussed in Sec. V below.

When studying a given process one also needs to take into account contributions from pion loops, which produce divergences that are eliminated by a renormalization of the low-energy constants of the effective Lagrangian. We have computed this divergent part of the one-loop generating

[3]The standard $\mathcal{O}(p^6)$ effective Lagrangian $\mathcal{L}^{(6)}=\mathcal{L}_{(6,0)}+\mathcal{L}_{(4,1)}+\mathcal{L}_{(2,2)}+\mathcal{L}_{(0,3)}$ has been worked out in Ref. [27] for the case of three light flavors, and very recently, for both two and three light flavors, in Ref. [28].

[4]For a review, see [29].

functional in the even intrinsic parity sector using standard heat-kernel techniques, and we have then performed the corresponding renormalization of the low-energy constants in the same dimensional renormalization scheme as described in [15,16]. Thus the low-energy constants display a logarithmic scale dependence [$X(\mu)$ denotes generically any of these renormalized low-energy constants]

$$X(\mu)=X(\mu')+\frac{\Gamma_X}{(4\pi)^2}\cdot\ln(\mu'/\mu). \tag{3.13}$$

The full list of the resulting β-function coefficients Γ_X is given in Appendix A. Let us however mention here that at order $\mathcal{O}(p^4)$ the low-energy constants of $\tilde{\mathcal{L}}^{(2)}$ and $\tilde{\mathcal{L}}^{(3)}$ also need to be renormalized. The corresponding counterterms, however, are of order $\mathcal{O}(B^2)$ and $\mathcal{O}(B)$, respectively, and they are gathered in the three last terms of Eq. (3.8): in GChPT, renormalization proceeds order by order in the expansion in powers of B. Alternatively, one may think of Eqs. (1.6) and (3.7) as standing for the combinations $\tilde{\mathcal{L}}^{(2)}+B^2\mathcal{L}'_{(0,2)}$ and $\tilde{\mathcal{L}}^{(3)}+B\mathcal{L}'_{(2,1)}+B\mathcal{L}'_{(0,3)}$, respectively, with the corresponding low-energy constants representing the renormalized, scale dependent quantities. We shall adopt the latter point of view in the following.

We have not worked out the general structure of the divergent part of the one-loop generating functional in the odd intrinsic parity sector. For SChPT, this has been done in Refs. [32,30,33].

IV. THE ONE-LOOP AMPLITUDES

Having constructed the effective Lagrangian in the preceding section, the computation of the amplitudes $\mathcal{A}^N$ and $\mathcal{A}^C$ at next-to-leading order becomes a straightforward exercise. We begin with the one-loop expression of the neutral amplitude $\mathcal{A}^N$, whose structure at that level of the chiral expansion is given by Eq. (2.8), with

$$\begin{aligned}\mathcal{A}_1^N(k,k';p_1,p_2,p_3)=&\frac{\mathcal{A}^{\pi^0\to\gamma\gamma}\mathcal{A}^{00;00}(p_{12}^2,p_{13}^2,p_{23}^2)}{s-M_\pi^2}\\
&-\frac{e^2}{4\pi^2F_\pi^3}\Bigg\{\frac{1}{2}(\beta-1)+\frac{1}{2}\hat{m}t(\beta-3)-\alpha M_\pi^2t'-4\hat{m}^2t''-\gamma_{00}+\frac{1}{F_\pi^2}(\lambda_1+2\lambda_2)(s-3M_\pi^2)+\frac{1}{F_\pi^2}\bar{J}(p_{12}^2)\\
&\times\left[p_{12}^2-M_\pi^2+\frac{1}{3}(\alpha-1)M_\pi^2\right]+\frac{1}{F_\pi^2}\bar{J}(p_{13}^2)\left[p_{13}^2-M_\pi^2+\frac{1}{3}(\alpha-1)M_\pi^2\right]\\
&+\frac{1}{F_\pi^2}\bar{J}(p_{23}^2)\left[p_{23}^2-M_\pi^2+\frac{1}{3}(\alpha-1)M_\pi^2\right]+\frac{2}{F_\pi^2}[\bar{R}(p_{12}^2,k\cdot p_{12})+\bar{R}(p_{12}^2,k'\cdot p_{12})]\left[p_{12}^2-M_\pi^2\right.\\
&\left.+\frac{1}{3}(\alpha-1)M_\pi^2\right]+\frac{2}{F_\pi^2}[\bar{R}(p_{13}^2,k\cdot p_{13})+\bar{R}(p_{13}^2,k'\cdot p_{13})]\left[p_{13}^2-M_\pi^2+\frac{1}{3}(\alpha-1)M_\pi^2\right]\\
&+\frac{2}{F_\pi^2}[\bar{R}(p_{23}^2,k\cdot p_{23})+\bar{R}(p_{23}^2,k'\cdot p_{23})]\left[p_{23}^2-M_\pi^2+\frac{1}{3}(\alpha-1)M_\pi^2\right]\Bigg\},\end{aligned} \tag{4.1}$$

and

$$\mathcal{A}_2^N(k,k';p_1,p_2,p_3)=\frac{e^2}{2\pi^2F_\pi^5}\bar{R}(p_{12}^2,k\cdot p_{12})\left[p_{12}^2-M_\pi^2+\frac{1}{3}(\alpha-1)M_\pi^2\right]. \tag{4.2}$$

This second amplitude, which was absent at tree level, is entirely generated by the pion loops. The numerator of the contribution which develops a pole at $s=M_\pi^2$ in the expression (4.1) of $\mathcal{A}_1^N$ is given by the product of $\mathcal{A}^{\pi^0\to\gamma\gamma}$, which is related to the on-shell amplitude of the $\pi^0\to\gamma\gamma$ decay through $\mathcal{A}(\pi^0\to\gamma\gamma)=-t_1(k,\epsilon,k',\epsilon')\mathcal{A}^{\pi^0\to\gamma\gamma}$, times the amplitude $\mathcal{A}^{00;00}(p_{12}^2,p_{13}^2,p_{23}^2)$ of virtual π^0-π^0 scattering ($p_{12}^2+p_{13}^2+p_{23}^2=s+3M_\pi^2$). The expressions, at order $\mathcal{O}(p^6)$ and order $\mathcal{O}(p^4)$, respectively, of these amplitudes read

$$\mathcal{A}^{\pi^0\to\gamma\gamma}=\frac{e^2}{4\pi^2F_\pi}[1+\hat{m}t+M_\pi^2t'+\hat{m}^2t''+2\hat{m}^2a_3], \tag{4.3}$$

and

$$\mathcal{A}^{00;00}(p_{12}^2,p_{13}^2,p_{23}^2)=\frac{\alpha M_\pi^2}{F_\pi^2}+\frac{1}{F_\pi^4}(\lambda_1+2\lambda_2)[(p_{12}^2-2M_\pi^2)^2+(p_{13}^2-2M_\pi^2)^2+(p_{23}^2-2M_\pi^2)^2]$$
$$+\frac{1}{F_\pi^4}\bar{J}(p_{12}^2)\left[\left(p_{12}^2-\frac{4}{3}M_\pi^2+\frac{\alpha}{3}M_\pi^2\right)^2+\frac{\alpha^2}{2}M_\pi^4\right]+\frac{1}{F_\pi^4}\bar{J}(p_{13}^2)\left[\left(p_{13}^2-\frac{4}{3}M_\pi^2+\frac{\alpha}{3}M_\pi^2\right)^2+\frac{\alpha^2}{2}M_\pi^4\right]$$
$$+\frac{1}{F_\pi^4}\bar{J}(p_{23}^2)\left[\left(p_{23}^2-\frac{4}{3}M_\pi^2+\frac{\alpha}{3}M_\pi^2\right)^2+\frac{\alpha^2}{2}M_\pi^4\right]. \tag{4.4}$$

The various parameters α, β, $\lambda_{1,2}$, and γ_{00} involved in the expressions (4.1) and (4.4) are given in terms of combinations of the low-energy constants of the effective Lagrangian $\mathcal{L}^{\text{eff}}$, displayed in Sec. III and in Appendix A, and of chiral logarithms due to the pion loops. They read

$$\frac{F_\pi^2}{F^2}M_\pi^2\alpha=2\hat{m}B+16\hat{m}^2A$$
$$+\hat{m}^3(81\rho_1^{(2)}+\rho_2^{(2)}+164\rho_4^{(2)}+2\rho_5^{(2)})-4M_\pi^2\hat{m}\xi^{(2)}+16\hat{m}^4(16e_1+e_2+32f_1+34f_2+2f_3+72f_4+6a_3A)$$
$$-8M_\pi^2\hat{m}^2(2b_1-2b_2-a_3-4c_1)-\frac{1}{16\pi^2F_\pi^2}[2M_\pi^4+102\hat{m}^2M_\pi^2A+264\hat{m}^4A^2]\ln\frac{M_\pi^2}{\mu^2}$$
$$-\frac{1}{16\pi^2F_\pi^2}\left[\frac{M_\pi^4}{2}+44\hat{m}^2M_\pi^2A+264\hat{m}^4A^2\right], \tag{4.5}$$

$$\beta=1+2\hat{m}\xi^{(2)}-4\hat{m}^2(\xi^{(2)})^2+2\hat{m}^2(3a_2+2a_3+4b_1+2b_2+4c_1)-\frac{M_\pi^2}{48\pi^2F_\pi^2}\left(\ln\frac{M_\pi^2}{\mu^2}+1\right)[6+5(\alpha-1)], \tag{4.6}$$

$$\lambda_1=\frac{1}{48\pi^2}\left(\bar{l}_1-\frac{4}{3}\right), \tag{4.7}$$

$$\lambda_2=\frac{1}{48\pi^2}\left(\bar{l}_2-\frac{5}{6}\right),$$

$$\gamma_{00}=\hat{m}^2(3a_2+2a_3+6b_2+12c_1)$$
$$-\frac{M_\pi^2}{32\pi^2F_\pi^2}\left(\ln\frac{M_\pi^2}{\mu^2}+1\right)(\alpha-1). \tag{4.8}$$

The parameters t, t', and t'' contain the contributions from $\mathcal{L}^-_{(4,1)}$, $\mathcal{L}^-_{(6,0)}$ and $\mathcal{L}^-_{(4,2)}$, respectively. In particular, from the formulas (3.11) and (3.12) we derive

$$t=\frac{32}{3}A_4,$$

$$t'=-\frac{8}{3}(A_2-2A_3). \tag{4.9}$$

Finally, $\bar{J}(s)$ denotes the Chew-Mandelstam function [34], the usual scalar two-point loop integral subtracted at $s=0$ (for its expression, see Ref. [15]), whereas $\bar{R}(p^2;k\cdot p)$, which is related to the three-point scalar loop function, is given, for $k^2=0$, by

$$\bar{R}(p^2;k\cdot p)=\bar{C}(p^2,k\cdot p)-\frac{(k-p)^2}{4(k\cdot p)}[\bar{J}((k-p)^2)-\bar{J}(p^2)]$$
$$+\frac{1}{32\pi^2}, \tag{4.10}$$

with ($\sigma=\sqrt{1-4M_\pi^2/p^2}$, $\sigma'=\sqrt{1-4M_\pi^2/(k-p)^2}$)

$$16\pi^2\bar{C}(p^2,k\cdot p)=\frac{M_\pi^2}{4(k\cdot p)}\left[\ln^2\left(\frac{\sigma-1}{\sigma+1}\right)-\ln^2\left(\frac{\sigma'-1}{\sigma'+1}\right)\right]. \tag{4.11}$$

For the charged amplitude $\mathcal{A}^C$, the general structure is more involved, see Eq. (2.6), and at one loop we obtain

$$\mathcal{A}_1^C(k,k';p_0,p_+,p_-)=\frac{\mathcal{A}^{\pi^0\to\gamma\gamma}\mathcal{A}^{00;+-}(p_{+-}^2,p_{+0}^2,p_{-0}^2)}{s-M_\pi^2}$$
$$+\frac{e^2}{4\pi^2F_\pi^3}\left\{\frac{1}{2}(\beta+1)+\frac{1}{2}\hat{m}t(\beta-1)-\frac{1}{3}(\alpha-1)M_\pi^2t'+\gamma_{+-}+\frac{2}{3}\gamma'_{+-}+\frac{\lambda_1}{F_\pi^2}(p_{+-}^2-2M_\pi^2)\right.$$
$$+\frac{1}{F_\pi^2}\left(\lambda_2-\frac{1}{288\pi^2}\right)(p_{+0}^2+p_{-0}^2-4M_\pi^2)+\frac{1}{6F_\pi^2}\overline{J}(p_{+-}^2)[3p_{+-}^2+4(\alpha-1)M_\pi^2]$$
$$\left.+\frac{1}{12F_\pi^2}\overline{J}(p_{+0}^2)[5p_{+0}^2-14M_\pi^2-2(\alpha-1)M_\pi^2]+\frac{1}{12F_\pi^2}\overline{J}(p_{-0}^2)[5p_{-0}^2-14M_\pi^2-2(\alpha-1)M_\pi^2]\right\},\tag{4.12}$$

$$\mathcal{A}_2^C(k,k';p_0,p_+,p_-)=\frac{e^2}{24\pi^2F_\pi^3}\left\{6+6\gamma'_{+-}-\frac{1}{48\pi^2F_\pi^2}[(k'-p_0)^2+p_{+0}^2+p_{-0}^2]-\frac{1}{F_\pi^2}\overline{J}(p_{+0}^2)[4M_\pi^2-p_{+0}^2]\right.$$
$$\left.-\frac{1}{F_\pi^2}\overline{J}(p_{-0}^2)[4M_\pi^2-p_{-0}^2]-\frac{1}{F_\pi^2}\overline{J}((k'-p_0)^2)[4M_\pi^2-(k'-p_0)^2]\right\},\tag{4.13}$$

$$\mathcal{A}_3^C(k,k';p_0,p_+,p_-)=-\frac{e^2}{4\pi^2F_\pi^5}\overline{R}(p_{+-}^2;k\cdot p_{+-})\left[p_{+-}^2+\frac{4}{3}(\alpha-1)M_\pi^2\right],\tag{4.14}$$

$$\mathcal{A}_4^C(k,k';p_0,p_+,p_-)=-\frac{e^2}{4\pi^2F_\pi^5}\left\{\frac{1}{3}\overline{J}((k'-p_-)^2)M_\pi^2\left(4\frac{k\cdot p_+}{k\cdot p_{+0}}-1\right)+\frac{1}{6}[\overline{J}((k'-p_-)^2)-\overline{J}(p_{+0}^2)]\left[p_{+0}^2+2M_\pi^2\right.\right.$$
$$+\frac{1}{2}\frac{p_{+0}^2}{k\cdot p_{+0}}(4M_\pi^2-p_{+0}^2)+\frac{k\cdot p_+}{k\cdot p_{+0}}(4M_\pi^2-7p_{+0}^2+6k\cdot p_{+0})+2\frac{k\cdot p_+}{k\cdot p_{+0}}\frac{p_{+0}^2}{k\cdot p_{+0}}(p_{+0}^2-4M_\pi^2)\Big]$$
$$+\overline{R}(p_{+0}^2;k\cdot p_{+0})\left[-M_\pi^2+2k\cdot p_+\left(\frac{p_{+0}^2}{k\cdot p_{+0}}-1\right)-\frac{1}{3}(\alpha-1)M_\pi^2\right]+\frac{1}{24\pi^2}k\cdot p_+\left(1-\frac{p_{+0}^2}{k\cdot p_{+0}}\right)$$
$$\left.+\frac{1}{96\pi^2}p_{+0}^2\right\},\tag{4.15}$$

$$\mathcal{A}_5^C(k,k';p_0,p_+,p_-)=-\frac{e^2}{24\pi^2F_\pi^5}\left\{\overline{J}((k'-p_-)^2)[4M_\pi^2-(k'-p_-)^2]-\overline{J}(p_{+0}^2)(4M_\pi^2-p_{+0}^2)-\frac{1}{24\pi^2}k\cdot p_{+0}\right\},\tag{4.16}$$

$$\mathcal{A}_6^C(k,k';p_0,p_+,p_-)=-\frac{e^2}{4\pi^2F_\pi^5}\left\{\frac{1}{6}[\overline{J}((k'-p_-)^2)-\overline{J}(p_{+0}^2)]\left[p_{+0}^2-4M_\pi^2-6k\cdot p_++4\frac{k\cdot p_+}{k\cdot p_{+0}}(p_{+0}^2-M_\pi^2)\right.\right.$$
$$\left.+\frac{k\cdot p_+}{(k\cdot p_{+0})^2}p_{+0}^2(4M_\pi^2-p_{+0}^2)\right]-\frac{1}{3}\overline{J}((k'-p_-)^2)\left[k\cdot p_0+2M_\pi^2\frac{k\cdot p_+}{k\cdot p_{+0}}\right]+\overline{R}(p_{+0}^2;(k-p_{+0})^2)(k\cdot p_+)$$
$$\left.\times\left[2-\frac{p_{+0}^2}{k\cdot p_{+0}}\right]+\frac{1}{32\pi^2}\frac{k\cdot p_+}{k\cdot p_{+0}}(k'-p_-)^2+\frac{1}{96\pi^2}\left(\frac{4}{3}k\cdot p_+-p_{+0}^2\frac{k\cdot p_+}{k\cdot p_{+0}}\right)+\frac{1}{144\pi^2}k\cdot p_{+0}\right\}.\tag{4.17}$$

The amplitude A_1^C again contains a contribution with a pole at $s=M_\pi^2$, which is given by the product of the $\mathcal{O}(p^6)$ $\pi^0\to\gamma\gamma$ amplitude $\mathcal{A}^{\pi^0\to\gamma\gamma}$ times the (off-shell) $\pi^0\pi^0\to\pi^+\pi^-$ amplitude $\mathcal{A}^{00;+-}$, with

$$-\mathcal{A}^{00;+-}(p_{+-}^2,p_{+0}^2,p_{-0}^2)=\frac{\beta}{F_\pi^2}\left(p_{+-}^2-\frac{4}{3}M_\pi^2\right)+\frac{1}{3F_\pi^2}\alpha M_\pi^2+\frac{\lambda_1}{F_\pi^4}(p_{+-}^2-2M_\pi^2)^2+\frac{\lambda_2}{F_\pi^4}[(p_{+0}^2-2M_\pi^2)^2+(p_{0-}^2-2M_\pi^2)^2]$$
$$+\frac{1}{6F_\pi^4}\overline{J}(p_{+-}^2)\left[4\left(p_{+-}^2-\frac{4}{3}M_\pi^2+\frac{5}{6}\alpha M_\pi^2\right)^2-\left(p_{+-}^2-\frac{4}{3}M_\pi^2-\frac{2}{3}\alpha M_\pi^2\right)^2\right]$$
$$+\frac{1}{12F_\pi^4}\overline{J}(p_{+0}^2)\left[3\left(p_{+0}^2-\frac{4}{3}M_\pi^2-\frac{2}{3}\alpha M_\pi^2\right)^2+(p_{+-}^2-p_{-0}^2)(p_{+0}^2-4M_\pi^2)\right]$$
$$+\frac{1}{12F_\pi^4}\overline{J}(p_{-0}^2)\left[3\left(p_{-0}^2-\frac{4}{3}M_\pi^2-\frac{2}{3}\alpha M_\pi^2\right)^2+(p_{+-}^2-p_{+0}^2)(p_{-0}^2-4M_\pi^2)\right], \tag{4.18}$$

where $p_{+-}^2+p_{+0}^2+p_{-0}^2=s+3M_\pi^2$.

The remaining parameters γ_{+-} and γ'_{+-} which appear in the amplitudes $\mathcal{A}_1^C$, ... $\mathcal{A}_6^C$ contain the contributions from the low-energy constants and chiral logarithms

$$\gamma_{+-}=-\hat{m}^2(a_2+2b_2+4c_1)+\frac{M_\pi^2}{96\pi^2F_\pi^2}\ln\frac{M_\pi^2}{\mu^2}(\alpha-1)$$
$$+\frac{M_\pi^2}{96\pi^2F_\pi^2}\left(\alpha-\frac{7}{3}\right)+\hat{m}^2\delta\gamma_{+-}, \tag{4.19}$$

$$\gamma'_{+-}=8\hat{m}(2A_{12}-A_{13})+8M_\pi^2(A_7-A_8)$$
$$+6\hat{m}^2a_3-\frac{M_\pi^2}{32\pi^2F_\pi^2}\ln\frac{M_\pi^2}{\mu^2}+\hat{m}^2\delta\gamma'_{+-}. \tag{4.20}$$

With the expressions given above, it is straightforward to check that the three conditions listed before Eq. (2.9) as well as Eq. (2.10) are satisfied, which provides a nontrivial check of our calculation. The isospin relation (2.9) implies that the condition

$$2+3\gamma_{+-}+\gamma_{00}+\frac{M_\pi^2}{24\pi^2F_\pi^2}=\hat{m}^2(2a_3-3t'') \tag{4.21}$$

must hold. This requires that the contributions of the $\mathcal{L}_{(4,2)}^-$ counterterms to γ_{+-}, which we have denoted as $\hat{m}^2\delta\gamma_{+-}$ in the expression (4.19), have to satisfy

$$3t''+3\delta\gamma_{+-}=0. \tag{4.22}$$

The contributions of the $\mathcal{L}_{(4,2)}^-$ counterterms to γ'_{+-}, $\hat{m}^2\delta\gamma'_{+-}$ in the expression (4.20), are not constrained by isospin symmetry.

Upon using the information provided by Table III in Appendix A, it is straightforward to check that α, β, and γ_{00} are scale independent by themselves (the parameters λ_1 and λ_2 were directly expressed in terms of the scale independent quantities $\overline{l}_1$ and $\overline{l}_2$ defined in Ref. [15]). In order for the amplitudes $\mathcal{A}^{\pi^0\to\gamma\gamma}$, $\mathcal{A}^N$, and $\mathcal{A}^C$ to be independent of the subtraction scale μ, the parameters t, t', t'', γ_{+-} and γ'_{+-} must be separately scale independent. This requires that $\delta\gamma_{+-}$, and $\delta\gamma'_{+-}$ themselves are scale independent. Since we have not worked out the structure of the one-loop divergences of the generalized generating functional in the odd intrinsic parity sector, we could not perform these checks explicitly.

From the above formulas, one may infer the expressions of the amplitudes in the standard case [25,26]. Since only the result for the neutral amplitude $\mathcal{A}^N$ was displayed explicitly in Ref. [25], and the expressions of the amplitudes $\mathcal{A}_i^C$ in the charged channel are only available from the unpublished work [26], we describe in some detail the necessary steps to obtain them. Their general structure is of course unchanged, the differences occur only in the expressions of the various combinations of low-energy constants that are involved. In particular, the contributions from $\mathcal{L}_{(0,3)}$, $\mathcal{L}_{(2,2)}$, $\mathcal{L}_{(0,4)}$, and $\mathcal{L}_{(4,2)}^-$ are relegated to higher orders. For the remaining constants, the correspondence with the usual SChPT notation is given as follows:

$$\hat{m}\xi_{\rm st}^{(2)}=\frac{M_\pi^2}{16\pi^2F_\pi^2}\left(\overline{l}_4+\ln\frac{M_\pi^2}{\mu^2}\right),$$
$$\alpha_{\rm st}=1+\frac{M_\pi^2}{32\pi^2F_\pi^2}(4\overline{l}_4-3\overline{l}_3-1),$$
$$\beta_{\rm st}=1+\frac{M_\pi^2}{8\pi^2F_\pi^2}(\overline{l}_4-1),$$
$$\gamma_{00,\rm st}=0,$$
$$\gamma_{+-,\rm st}=-\frac{M_\pi^2}{72\pi^2F_\pi^2},$$
$$\gamma'_{+-,\rm st}=8M_\pi^2\left(A_7-A_8+\frac{2A_{12}-A_{13}}{2B}\right)$$
$$-\frac{M_\pi^2}{32\pi^2F_\pi^2}\ln\frac{M_\pi^2}{\mu^2}. \tag{4.23}$$

We have checked that upon substituting these expressions into the one-loop amplitudes $\mathcal{A}^N$ and $\mathcal{A}^C$ given above, we

recover the results of the standard case, up to the contributions from the counterterms contained in t and t', which were not included in Refs. [25,26].

V. COUNTERTERM ESTIMATES AND NUMERICAL RESULTS

In order to make numerical estimates for the cross sections based on the $\mathcal{O}(p^6)$ amplitudes, we first need to fix or estimate the values of the various counterterms involved.

(i) λ_1,λ_2. At order $\mathcal{O}(p^4)$, these parameters are related to $\overline{l}_1$ and $\overline{l}_2$ through Eq. (4.7). The values of these low-energy constants in the standard case have been the subject of numerous studies in the literature [15,35–38]. A first determination at order $\mathcal{O}(p^4)$ was given in Ref. [15], using information from the D-wave π-π scattering lengths. The corresponding values, taken from a recent numerical reanalysis [39], are

$$\overline{l}_{1,\mathrm{GL}}=-2.15\pm 4.30, \quad \overline{l}_{2,\mathrm{GL}}=5.84\pm 1.72, \tag{5.1}$$

leading to

$$\lambda_{1,\mathrm{GL}}=(-7.35\pm 9.06)\times 10^{-3},$$
$$\lambda_{2,\mathrm{GL}}=(10.57\pm 3.63)\times 10^{-3}. \tag{5.2}$$

The parameters λ_1 and λ_2 can also be determined directly, via a set of rapidly convergent sum-rules [40], from the knowledge, at two-loop order, of the π-π scattering amplitude $A(s|t,u)$ in GChPT [12], and from medium energy data on π-π phase shifts. The values obtained this way correspond to a determination at order $\mathcal{O}(p^6)$. They depend only very weakly on the values of the parameters α and β when the latter are varied within the ranges specified below, and read

$$\lambda_1=(-6.1\pm 2.2)\times 10^{-3}, \quad \lambda_2=(9.6\pm 0.5)\times 10^{-3}. \tag{5.3}$$

These values are compatible with those given in Eq. (5.2), but are affected by much smaller error bars. The analysis may even be refined in the standard case, using the information on the SChPT two-loop π-π amplitude obtained in Ref. [37], leading to the following values [38]:

$$\lambda_{1,\mathrm{st}}=(-5.7\pm 2.2)\times 10^{-3}, \quad \lambda_{2,\mathrm{st}}=(9.3\pm 0.5)\times 10^{-3}. \tag{5.4}$$

(ii) α,β. At leading order, α is directly correlated to the size of the condensate, see Eq. (1.12). As such, the value of α is not predicted by GChPT, but remains a free parameter, that can *a priori* be varied in the range $1\lesssim\alpha\lesssim 4$. At order $\mathcal{O}(p^4)$, the relationship between α and the ratio $2\hat{m}B/M_\pi^2$ becomes more complicated, as shown in Eq. (4.5). The corresponding next-to-leading and next-to-next-to leading corrections have been estimated in Ref. [12] (see in particular the Figs. 8 and 10 in that reference). Notice that the analysis of Ref. [12] was done within the framework of $SU(3)_L\times SU(3)_R$ chiral perturbation theory. Working with only two light flavors as in the present paper might further reduce the uncertainties in the correspondence between the value of α and the size of the condensate, due to the lower number of unknown counterterms involved, and due to the absence of large contributions from the chiral logarithms induced by the kaon loops [41]. However, the results of Ref. [12] are sufficient for our present purposes, and we shall not pursue that matter further. Once α is given, the parameter β is also constrained by low-energy π-π data. The correlation between α and β, which results from the Morgan-Shaw universal curve [42], has also been studied beyond leading order in [12], and is summarized in Fig. 6 of that reference. For the subsequent numerical analyses, we shall take the values given in Table I. The values given in the second line of this table correspond to the one-loop values α_{st} and β_{st} of the standard case, which follow from the expressions given in Eq. (4.23), and from the values $\overline{l}_3=2.9\pm 2.4$ [15], $\overline{l}_4=4.4\pm 0.3$ [43]. Two points are worth being remembered. The first is that, independently of the value of α, β stays close to unity. The second point is that the standard case allows us to make a very precise prediction for the value of α at order $\mathcal{O}(p^4)$, *viz.* $\alpha_{\mathrm{st}}=1.06\pm 0.06$. Furthermore, this value is barely affected by the corrections at order $\mathcal{O}(p^6)$: The analysis of Ref. [38], based on the results of [37], gives $\alpha_{\mathrm{st}}=1.07\pm 0.01$ and $\beta_{\mathrm{st}}=1.105\pm 0.015$ at next-to-next leading order. Therefore, any significant deviation of the value of α from unity would provide evidence for a departure from the standard scenario of chiral symmetry breaking with a strong condensate.

TABLE I. Values of β, γ_{00} and γ_{+-} for different values of α.

α	β	$\gamma_{00}\times 10^3$	$\gamma_{+-}\times 10^3$
1.06 ± 0.06	1.103 ± 0.008	0	-3
1.5	1.06 ± 0.06	8 ± 3	-5.7 ± 0.8
2	1.07 ± 0.06	16 ± 5	-8.4 ± 1.6
2.5	1.08 ± 0.06	24 ± 8	-11.0 ± 2.4
3	1.11 ± 0.06	32 ± 10	-13.7 ± 3.2

(iii) t,t',t''. The constants t, t', and t'' appear in the expression of the $\pi^0\to\gamma\gamma$ amplitude (4.3). The uncertainty on the experimental value of the decay rate [5], $\Gamma(\pi^0\to\gamma\gamma)=7.74\pm 0.56$ eV, only yields a very weak constraint on the combination that appears in $\mathcal{A}^{\pi^0\to\gamma\gamma}$, *viz.* $\hat{m}t+M_\pi^2 t'+\hat{m}^2 t''=(0.0\pm 3.6)\times 10^{-2}$. This is comparable to the estimate one would obtain through naive dimensional analysis [44]. In addition, as shown in Ref. [45], isospin breaking effects can be sizable in $\mathcal{A}^{\pi^0\to\gamma\gamma}$. Further information may be obtained by making use of the sum-rules considered in Ref. [45]. The corrections due to t' were however not taken into account there, but the analysis of [45] is easily extended to the more general situation. In the generalized case, a similar set of sum rules can be established, but they do not yield complete information on the three constants t, t', and t''. We have summarized this analysis in Appendix B for the interested reader. Here, we only quote the values that we shall use in the sequel (the estimate for t'' follows from naive dimensional analysis),

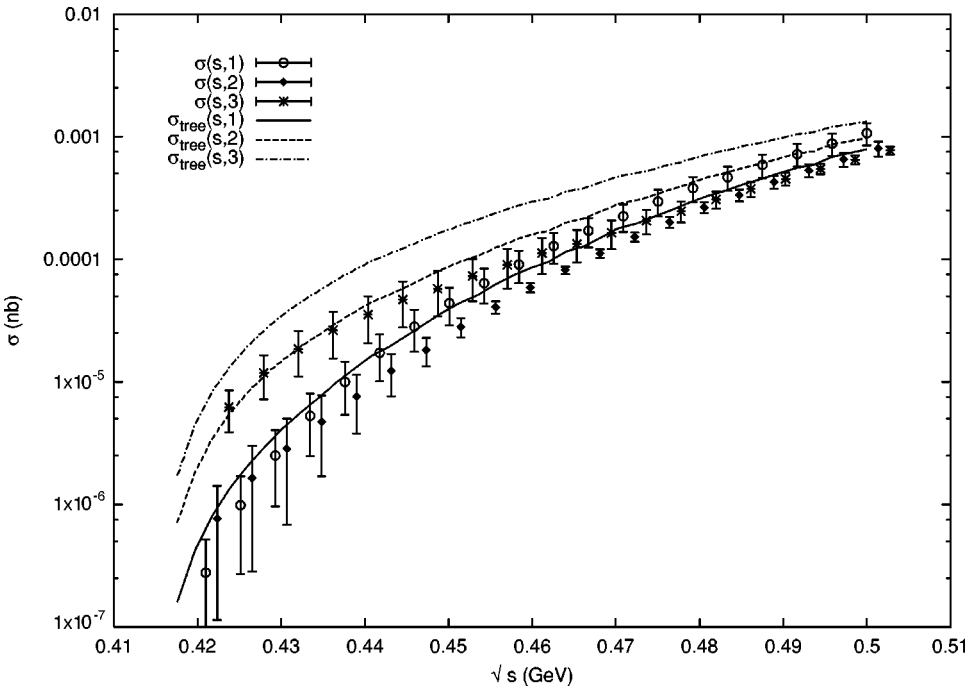

FIG. 2. The cross section $\sigma^C(s,\alpha)$ (in logarithmic scale) for $\gamma\gamma\to\pi^+\pi^-\pi^0$ as a function of the center of mass total energy, for three values of α, compared to the corresponding curves for the tree level cross section $\sigma^C_{\rm tree}(s,\alpha)$.

$$\hat{m}t=(6\pm12)\times10^{-3},\quad M_\pi^2t'=(-3\pm3)\times10^{-3},$$

$$\hat{m}^2t''\sim\pm1\times10^{-3}. \tag{5.5}$$

(iv) $\gamma_{00},\gamma_{+-},\gamma'_{+-}$. The main difficulty in obtaining numerical estimates for these parameters comes from the lack of knowledge, in the generalized case, on the contributions from the low-energy constants of $\mathcal{L}^+_{(2,2)}$. In the spirit of vector meson dominance (VMD), we have estimated the contributions of vector mesons to the two amplitudes $\mathcal{A}^N$ and $\mathcal{A}^C$, as done in Ref. [25] for the standard case. This way, we find that t, t' and t'' receive no contribution, whereas the contribution to γ_{00}, γ_{+-}, and γ'_{+-} read

$$\gamma_{00}|_{\rm VMD}=\gamma_{+-}|_{\rm VMD}=0,\quad \gamma'_{+-}|_{\rm VMD}=-\frac{3}{4}\,\frac{M_\pi^2}{M_V^2}\sim-0.024. \tag{5.6}$$

We take Eq. (5.6) as the values of these constants at the scale $\mu\sim M_V=770$ MeV, and estimate the error associated to the VMD approximation and to the presence of the low-energy constants from $\mathcal{L}^+_{(2,2)}$ in the expressions of γ_{00} and of γ_{+-} by varying the scale μ of the corresponding chiral logarithms between 500 MeV and 1 GeV. The resulting values for γ_{00} and γ_{+-} are shown in Table I. In the case of γ'_{+-}, we obtain a constant value which, to a very good precision, is compatible with zero.

With the above inputs at hand, we may now consider a few numerical applications. In Fig. 2, we have plotted the tree-level and one-loop cross sections for the charged channel, $\sigma^C_{\rm tree}(s,\alpha)$ and $\sigma^C(s,\alpha)$ in the threshold region $3M_\pi\leqslant\sqrt{s}\leqslant0.5$ GeV, where we expect the one-loop expression of the amplitude to be reliable, and for different values of α. We have used $M_{\pi^\pm}=M_{\pi^0}=135$ MeV in the amplitude and the experimental values, as quoted in [5], in the phase space integrals.

Let us first concentrate on the standard case ($\alpha\sim1$) which has been discussed before in the literature. In the energy region that we are considering, the correction as compared to the tree-level cross section does not exceed 30%, if we consider the central values, except very close to threshold, where it can reach 60%. This agrees with the unpublished result [26], but is much less than previously found in [25]. On the other hand, the error bars induced by the uncertainties attached to the various counterterm contributions that enter the $\mathcal{O}(p^6)$ amplitude are important. A closer analysis (see also below) reveals that the main contribution comes from the uncertainty on the value of λ_1 given in Eq. (5.4). This shows also that the sensitivity of the cross section on the $\mathcal{O}(p^6)$ counterterms becomes already sizable even at such low energies. Coming now to the dependence with respect to α, we see that here also the higher order corrections have a deep influence and upset the situation that prevailed at tree level. For $\alpha\geqslant2$ the one-loop cross sections are suppressed as compared to their tree-level values, and become even smaller than $\sigma^C(s,1)$ as the energy increases. The corrections to the tree-level results are largest in the vicinity of the threshold, where however the cross sections rapidly drop to zero. In the second half of the energy region shown in Fig. 2, the relative corrections in the cross sections amount to 50% or less, which is a typical size of one-loop effects. Unfortunately, the present theoretical error bars make it difficult to disentangle in practice the different situations, as far as the dependence on α is concerned, from the knowledge of the total cross section alone.

The cross sections $\sigma^N_{\rm tree}(s,\alpha)$ and $\sigma^N(s,\alpha)$ in the neutral channel have been plotted in Fig. 3. Whereas $\sigma^N_{\rm tree}(s,\alpha)\sim\alpha^2$, the corrections are seen to have an even more drastic

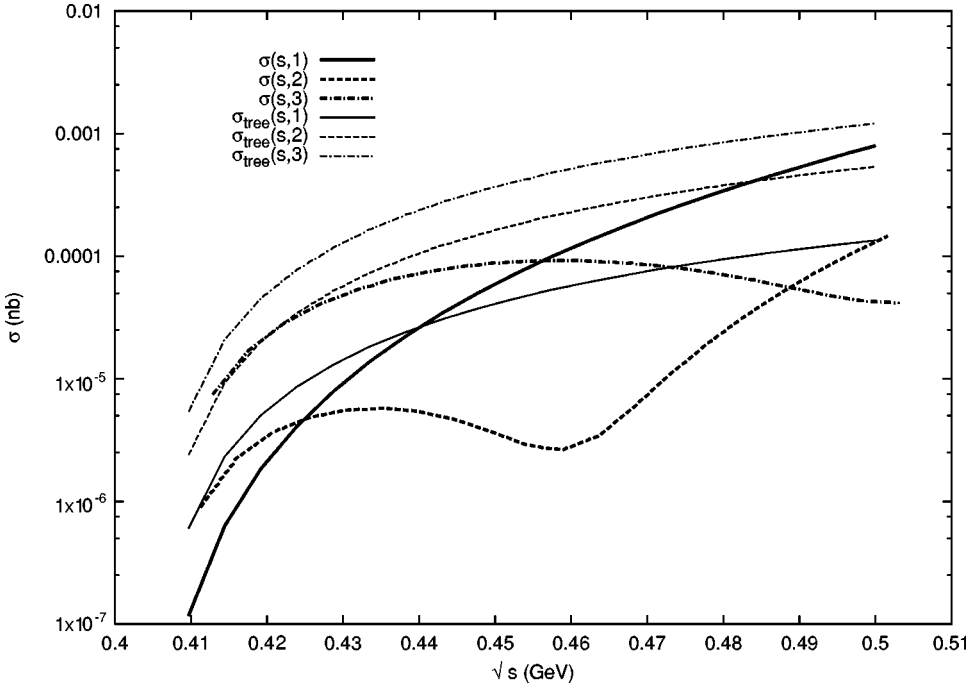

FIG. 3. The cross section $\sigma^N(s,\alpha)$ (in logarithmic scale) for $\gamma\gamma\to\pi^0\pi^0\pi^0$ as a function of the center of mass total energy, for three values of α. Also shown are the corresponding curves for the tree-level cross section $\sigma^N_{\rm tree}(s,\alpha)$.

influence on the behavior of the cross section as a function of energy than in the charged channel. Unfortunately, as far as the dependence on α is concerned, the picture is again totally blurred by the uncertainties, which, for the sake of clarity, we have not shown, but which are even more important than in the charged case. On the other hand, the loop corrections to the tree-level cross sections are very large, even at small energies. One might think of ascribing this feature to the fact that, contrary to the charged channel, the neutral process is described by a single amplitude at tree level, while the loop corrections bring in additional amplitudes, which might then result into similar destructive interference effects as in the charged case. However, this would still require that the one-loop corrections be comparable to the tree-level contributions.

Actually, this happens to be the case, as follows from Fig. 4, where the cross sections obtained by taking into account the contributions from $\mathcal{A}^N_1$ only have been plotted for different values of α. While the error bars are now small enough in order to distinguish the α dependence, the one-loop corrections however are indeed very important, and a closer analysis reveals that they are almost completely dominated by the contribution of the pole part in Eq. (4.1), given by the off-shell amplitude $\mathcal{A}^{00;00}$ displayed in Eq. (4.4). At tree

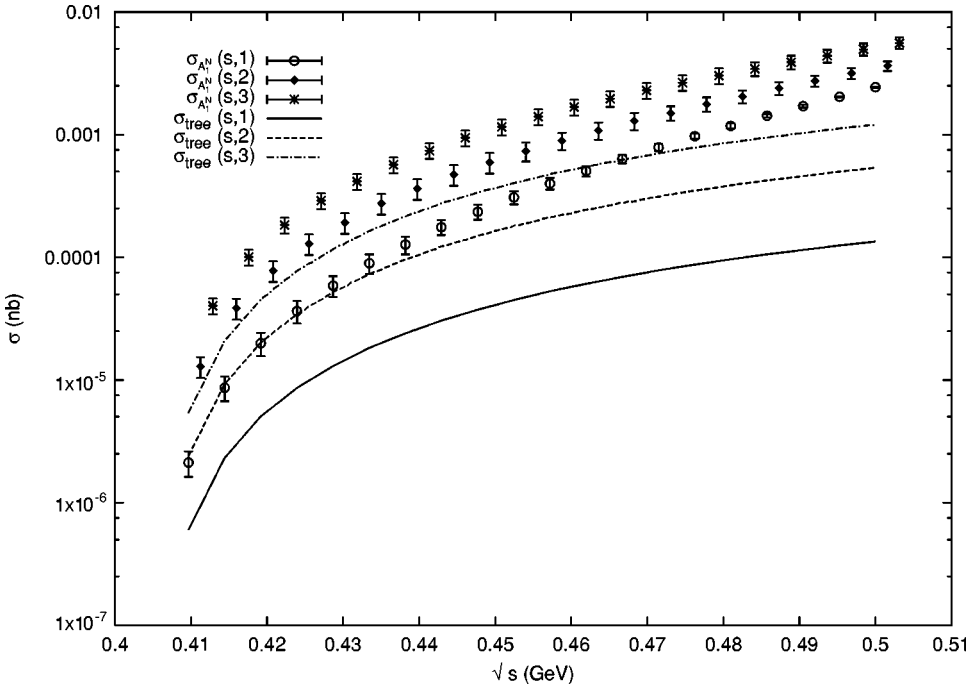

FIG. 4. The cross section $\sigma_{A^N_1}(s,\alpha)$ for $\gamma\gamma\to\pi^0\pi^0\pi^0$ obtained by taking into account the contribution from the amplitude A^N_1 alone, for different values of α.

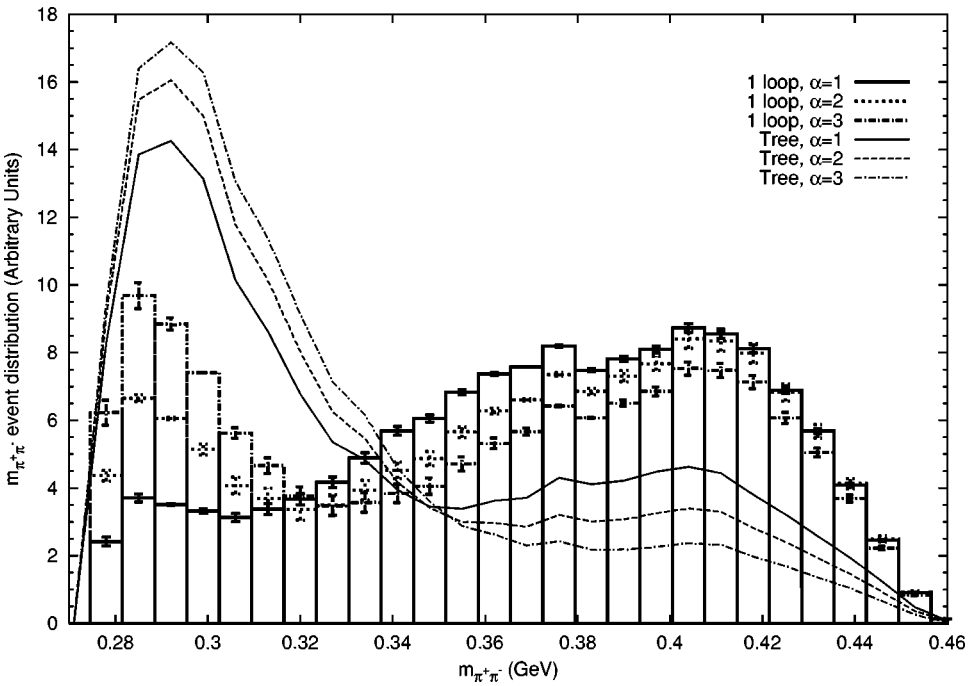

FIG. 5. The histogram of the distribution of the invariant mass $m_{\pi^+\pi^-}$ of the two final charged pions in the process $\gamma\gamma \to \pi^+\pi^-\pi^0$ for different values of α and $\sqrt{s} \leq E_{\max} = 0.6$ GeV. Also shown are the curves corresponding to the same distribution, but from the lowest order amplitude alone.

level, this amplitude is constant and given by $\alpha M_\pi^2/F_\pi^2$. At threshold ($p_{12}^2 = p_{23}^2 = p_{13}^2 = 4M_\pi^2$), the corrections to this tree-level value represent 110% for $\alpha = 1$, 70% for $\alpha = 2$, and 60% for $\alpha = 3$, and they are dominated by the momentum dependences which arise at the one-loop level (the corrections induced by λ_1 and λ_2 alone do not exceed 30%). As one moves away from threshold, these corrections to $Re\mathcal{A}^{00;00}$, which remain always positive, become even larger. At this stage, it is hard, without doing an explicit calculation much beyond the scope of the present work, to assess the effects of higher order corrections on $\sigma^N(s,\alpha)$. On the other hand, if we consider what happens for the on-shell $\pi^0\pi^0 \to \pi^0\pi^0$ amplitude, which is given, at the $\pi^0\pi^0$ threshold $p_{12}^2 = 4M_\pi^2$, $p_{23}^2 = p_{14}^2 = 0$, by the combination $a_0^0 + 2a_0^2$ of $\pi - \pi$ scattering lengths a_l^I, we can at least see a possibility why these corrections could be small after all. For $\alpha = 1$, the one-loop corrections represent an increase of 60% in the value of the $a_0^0 + 2a_0^2$, whereas they only amount to 25% for a_0^0 and to less than 5% for a_0^2 [15]. The two-loop corrections to $a_0^0 + 2a_0^2$ are however small, around 6% for $\alpha = 1$ [37,38]. Similar statements can be made for different values of α and/or for the behavior of the cross section for elastic scattering of neutral pions in the low-energy domain.

Thus, in both channels the origin of the large error bars is a consequence of the highly destructive interferences between the various amplitudes. In the charged case, this interference was already present at tree level, and is even somewhat enhanced by the loop effects. In the neutral case, the strong α dependence of the single amplitude that contributes at lowest order is, in a similar way, washed out by the interferences between the two one-loop amplitudes $\mathcal{A}_1^N$ and $\mathcal{A}_2^N$. In the latter case, the importance of the interference effects with the second amplitude $\mathcal{A}_2^N$ appears clearly upon comparing Figs. 3 and 4 (for the standard case, a similar observation was already made by the authors of Ref. [25]). Unfortunately, we have not found a simple way to extract the contribution from $\mathcal{A}_1^N$ only; for photons with perpendicular polarizations, the two amplitudes contribute, and the destructive interference between them is again at work, while for photons with parallel polarizations, only the very small contribution from $\mathcal{A}_2^N$, which vanishes at tree level, is singled out. We have therefore tried to investigate whether looking at more refined observables than the total cross sections allows us to reach better perspectives from the point of view of the dependence with respect to α. We have, for instance, considered the invariant mass distribution of the two charged pions in the $\gamma\gamma \to \pi^+\pi^-\pi^0$ channel. The result is shown in Fig. 5. As one may observe, the error bars are much less important than for the total cross section, and the different values of α can be distinguished over a substantial portion of the energy range that has been considered. Actually, analyses of this type usually require sufficiently high statistics, which also represents a problem in the present case.

Indeed, in both channels, the cross sections are very small at low energies, orders of magnitude below, for instance, the corresponding cross sections for the $\gamma\gamma \to \pi\pi$ processes. We have therefore also estimated the numbers of events that could be expected at an $e^+ - e^-$ collider for the two-photon total invariant mass $\sqrt{s}$ below a maximal energy $E_{\max}$. As typical examples, we have considered two instances of symmetric $e^+ - e^-$ colliders. The first case corresponds to the Daphne ϕ-factory [21], with a total beam energy of $E_{\text{beam}} = 510$ MeV, and a nominal integrated luminosity of 5×10^6 nb^{-1} per year. The second case concerns a τ-charm factory configuration [46], with a beam energy four times as large as for Daphne, and a design integrated luminosity of 10^7 nb^{-1} per year. The numbers of events are obtained upon convoluting the above cross sections with the corresponding photon luminosities quoted in [47] (since we are not inter-

TABLE II. Number of events for $\gamma\gamma\to\pi^+\pi^-\pi^0$ and for $\gamma\gamma\to\pi^0\pi^0\pi^0$ at a τ-charm factory as a function of the maximal energy $E_{\max}$ (GeV), and the principal sources of error.

Mode	$E_{\max}$ (GeV)	α	#events	Δ(#events)	$\Delta\lambda_1$	$\Delta\lambda_2$	$\Delta\beta$	$\Delta\hat{m}t$
		1	16	4	3.3	1.3	0.3	1.3
	0.50	2	11	1	1	0.2	0.2	0.4
		3	12	2	1	0.6	1.8	0.5
		1	56	11	9.7	3.6	0.6	3.5
$\pi^+\pi^-\pi^0$	0.55	2	40	5	4.5	1.3	0.1	1.8
		3	38	3	0.2	0.6	3.1	0.1
		1	327	56	50	18	1.8	14
	0.60	2	273	39	35	11	2.7	10
		3	246	26	24	5.7	4.4	7.3
		1	14	7	5.9	2.7	0.7	2.3
	0.50	2	1	2	1.2	0.6	1	0.5
		3	5	4	2.6	1.2	2.6	1.3
		1	42	18	15.8	7.2	1.8	5.6
$\pi^0\pi^0\pi^0$	0.55	2	8	9	5.9	2.7	4.8	2.1
		3	6	3	1.7	0.8	2.0	1.0
		1	211	81	71	32	6.3	19
	0.60	2	91	59	45	20	28	12
		3	51	34	26	12	15	6.6

ested in resonant η production, whenever necessary we avoided the η peak by applying a cut on $m_{\gamma\gamma}$ such that only the events with $m_{\gamma\gamma}<M_\eta-\Delta$ or $m_{\gamma\gamma}>M_\eta+\Delta$, with $\Delta=20$ MeV are accepted),

$$\frac{dL_{\gamma\gamma}}{dm_{\gamma\gamma}}=\frac{4}{m_{\gamma\gamma}}\left(\frac{\alpha}{\pi}\ln\frac{E_{\rm beam}}{m_e}\right)^2 \times[-(2+z^2)^2\ln z-(1-z^2)(3+z^2)], \quad (5.7)$$

where $m_{\gamma\gamma}=\sqrt{s}$ is the photon-photon center of mass energy, $z=m_{\gamma\gamma}/2E_{\rm beam}$, and m_e is the electron mass. For the luminosity quoted above, the expected total number of $\gamma\gamma\to\pi^+\pi^-\pi^0$ events per year at energies $\sqrt{s}\lesssim 0.6$ GeV is around 5 ± 1 for Daphne (independently of α) and even less in the neutral case. In the case of a τ-charm factory, the total number of events becomes sizable, and the results are shown, for the two modes, in the fourth column of Table II, for different choices of $E_{\max}$ (second column) and for different values of α (third column). Also shown are the corresponding uncertainties Δ(#events) (fifth column), while the remaining entries show various sources of contributions to the total error Δ(#events). The latter was obtained upon adding the individual contributions in quadrature. As mentioned above, the main source of error comes from the uncertainty on the value of λ_1. A sizable but not necessarily drastic reduction of the latter would already allow us to distinguish the standard case of a strong condensate ($\alpha\sim1$) from situations where spontaneous breakdown of chiral symmetry would be triggered by a much weaker condensate ($\alpha\gtrsim2$).

VI. SUMMARY AND CONCLUSIONS

In the present paper, the amplitudes of the processes $\gamma\gamma\to\pi^0\pi^0\pi^0$ and $\gamma\gamma\to\pi^+\pi^-\pi^0$ have been computed in the framework of $SU(2)_L\times SU(2)_R$ generalized chiral perturbation theory to $\mathcal{O}(p^6)$ precision. The corresponding generating functional has been constructed explicitly in Sec. III (see also Appendix A), and the structure of its divergences in the sector of even intrinsic parity has been analyzed. The resulting amplitudes, worked out in Sec. IV, satisfy the isospin relations that we have established in Sec. II (to the best of our knowledge, these relations have not been discussed previously in the literature). When restricted to the standard case, specified by the choice of parameters as indicated in Eq. (4.23), we recover the results obtained by previous authors [25,26], both in the neutral and in the charged case. Finally, we have estimated the counterterms that enter the one-loop amplitudes and we have performed some numerical analyses in Sec. V.

As far as the chiral corrections to the total cross sections are concerned, we have found them to be of the typical size of one-loop effects in the charged channel. It is thus reassuring that the delicate balance which leads to the highly destructive interference effects between the two amplitudes $\mathcal{A}_1^C$ and $\mathcal{A}_2^C$ at tree level is not too strongly affected by the one-loop corrections. One may therefore expect that higher order contributions will only induce small corrections. In the neutral channel, where we have found that the one-loop corrections are large, the situation with respect to higher order corrections appears as less reliable. These important one-loop effects can be ascribed to the peculiarities of the amplitude $\mathcal{A}^{00;00}(s,t,u)$, for which the two-loop corrections are however very small, at least in the physical region for elastic low-energy $\pi^0\pi^0\to\pi^0\pi^0$ scattering. We have also shown that the uncertainties associated with the counterterm estimates induce, through the destructive interferences between the various amplitudes that build up the total cross sections, large error bars, especially in the neutral channel.

We have then considered the possible detection of these processes at Daphne and at a τ-charm factory. Unfortunately, the expected number of events is rather discouraging in the first case. Depending on the actual values of the counterterms and on α, it is hard to expect more than ~ 5 events per year with total invariant mass lower than 500 MeV. The number of events increases substantially when allowing larger invariant masses, but at the expense of working in an energy region where the $\mathcal{O}(p^6)$ expressions are probably less reliable, since higher order terms can become important even in the charged case. The computation at order $\mathcal{O}(p^8)$ would provide a better control of higher orders, and would also allow us to work at somewhat higher energies, thus leading to a substantial increase of the number of events already at Daphne. The required amount of work seems excessive, though, and would make sense only if conducted in parallel with a better determination of $\overline{l}_1$ (for instance, from a two-loop analysis of K_{l4} decays), by far the main source of theoretical uncertainties at present. We rather expect interesting and realistic prospects in this field to come from future machines, like the τ-charm factory, which run at higher energy and higher luminosity.

ACKNOWLEDGMENTS

We are pleased to thank A. Bramon for discussions and for his interest and collaboration at the early stages of this work, and J. Bijnens for discussions. One of us (M.K.) wishes to acknowledge clarifying correspondence and/or discussions with I. Kogan and J. Stern on the content of Ref. [8], and expresses his thanks to L. Girlanda for discussions and for sharing unpublished work. He also acknowledges the hospitality of the Universitat Politècnica de Catalunya and of the Universitat Autònoma de Barcelona. Ll.A. thanks the Institut de Physique Nucléaire in Orsay for its hospitality. P.T. expresses his gratitude to the FEN department, where most of his contribution to the present work was done. This work was partially supported by the TMR Program, EC-Contract No. CT98-0169. Ll.A. and P.T. received support from the CICYT research project No. AEN95-0815, while the work of J.K. and of P.T. was supported by the Schweizerischer Nationalfonds and by the Swedish Research Council (NFR), respectively.

APPENDIX A

In the present appendix, we give the remaining pieces of the effective Lagrangian of GChPT at order $\mathcal{O}(p^4)$. The part with two powers of momenta and two powers of quark masses is given by

$$\begin{aligned}\mathcal{L}_{(2,2)}=&\frac{1}{4}F^2\{a_1\langle D_\mu U^+ D^\mu U(\chi^+\chi+U^+\chi\chi^+U)\rangle+a_2\langle D_\mu U^+ U\chi^+ D^\mu U U^+\chi\rangle+a_3\langle D_\mu U^+ U(\chi^+ D^\mu\chi-D^\mu\chi^+\chi)\\&+D_\mu U U^+(\chi D^\mu\chi^+-D^\mu\chi\chi^+)\rangle+b_1\langle D_\mu U^+ D^\mu U(\chi^+ U\chi^+ U+U^+\chi U^+\chi)\rangle+b_2\langle D_\mu U^+\chi D^\mu U^+\chi\\&+\chi^+ D_\mu U\chi^+ D^\mu U\rangle+b_3\langle U^+ D_\mu\chi U^+ D^\mu\chi+D_\mu\chi^+ U D^\mu\chi^+ U\rangle+c_1\langle D_\mu U^+\chi+\chi^+ D_\mu U\rangle\langle D^\mu U^+\chi+\chi^+ D^\mu U\rangle\\&+c_2\langle D_\mu\chi^+ U+U^+ D_\mu\chi\rangle\langle D^\mu U^+\chi+\chi^+ D^\mu U\rangle+c_3\langle D_\mu\chi^+ U+U^+ D_\mu\chi\rangle\langle D^\mu\chi^+ U+U^+ D^\mu\chi\rangle\\&+c_4\langle D_\mu U^+\chi-\chi^+ D_\mu U\rangle\langle D^\mu U^+\chi-\chi^+ D^\mu U\rangle+c_5\langle D_\mu\chi^+ U-U^+ D_\mu\chi\rangle\langle D^\mu\chi^+ U-U^+ D^\mu\chi\rangle+h_3\langle D_\mu\chi^+ D^\mu\chi^+\rangle\}.\end{aligned}\tag{A1}$$

The tree-level contributions which behave as $\mathcal{O}(m_{\text{quark}}^4)$ in the chiral limit are contained in $\mathcal{L}_{(0,4)}$, which reads

$$\begin{aligned}\mathcal{L}_{(0,4)}=&\frac{1}{4}F^2\{e_1\langle(\chi^+U)^4+(U^+\chi)^4\rangle+e_2\langle\chi^+\chi(\chi^+U\chi^+U+U^+\chi U^+\chi)\rangle+e_3\langle\chi^+\chi U^+\chi\chi^+U\rangle+f_1\langle(\chi^+U)^2+(U^+\chi)^2\rangle^2\\&+f_2\langle(\chi^+U)^3+(U^+\chi)^3\rangle\langle\chi^+U+U^+\chi\rangle+f_3\langle\chi^+\chi(\chi^+U+U^+\chi)\rangle\langle\chi^+U+U^+\chi\rangle+f_4\langle(\chi^+U)^2\\&+(U^+\chi)^2\rangle\langle\chi^+U+U^+\chi\rangle^2+f_5\langle(\chi^+U)^3-(U^+\chi)^3\rangle\langle\chi^+U-U^+\chi\rangle+h_4\langle\chi^+\chi\chi^+\chi\rangle+h_5\langle\chi^+\chi\rangle(\det\chi+\det\chi^+)\\&+h_6(\det\chi+\det\chi^+)^2+h_7(\det\chi-\det\chi^+)^2\}.\end{aligned}\tag{A2}$$

Finally, in Table III we also provide the list of β-function coefficients which describe the renormalization scale dependence of the various low-energy constants.[5]

APPENDIX B

In this appendix, we give a brief description of our analysis of the anomalous counterterms A_2, A_3, A_4, and A_6 which is based on the approach of Ref. [45]. The starting points are the invariant amplitudes $\Pi_{VVP}(p^2,q^2,r^2)$ and $\Pi^0_{VVP}(p^2,q^2,r^2)$ of

[5]These results have also been established independently by L. Girlanda, private communication, to M.K. and [41]. The renormalization of the $\mathcal{L}^+_{(4,0)}$ counterterms has, of course, already been obtained before in [15].

TABLE III. Scale dependence of the low energy constants.

X	$F^2\cdot\Gamma_X$	X	$F^2\cdot\Gamma_X$	X	Γ_X
A	$3B^2$	$\xi^{(2)}$	$4B$	l_1	$\frac{1}{3}$
Z^P	$-\frac{3}{2}B^2$	$\rho_1^{(2)}$	$-4B(A+Z^P)$	l_2	$\frac{2}{3}$
h_0	0	$\rho_2^{(2)}$	$-4B(A-3Z^P)$	l_5	$-\frac{1}{6}$
h_1	$6B^2$	$\rho_3^{(2)}$	$2B(A+3Z^P)$	l_6	$-\frac{1}{3}$
		$\rho_4^{(2)}$	$2B(3A+Z^P)$	h_2	$\frac{1}{12}$
		$\rho_5^{(2)}$	$4B(A-2Z^P)$		

X	$F^2\cdot\Gamma_X$	X	$F^2\cdot\Gamma_X$
a_1	$-2Z^P$	e_1	$-4A^2-22(Z^P)^2-20AZ^P$
a_2	$-12Z^P$	e_2	$-4A^2-16(Z^P)^2-12AZ^P$
a_3	0	e_3	$-12A^2-64(Z^P)^2-48AZ^P$
b_1	$6(A+Z^P)$	f_1	$3A^2+15(Z^P)^2+12AZ^P$
b_2	$-2(A+Z^P)$	f_2	$2A^2+8(Z^P)^2+10AZ^P$
b_3	0	f_3	$4A^2+24(Z^P)^2+20AZ^P$
c_1	$2(A+2Z^P)$	f_4	$-6(Z^P+A)Z^P$
c_2	0	f_5	$2A^2+8(Z^P)^2+10AZ^P$
c_3	0	h_4	$4A^2+8(Z^P)^2+8AZ^P$
c_4	$2A$	h_5	$-4A^2-32(Z^P)^2-28AZ^P$
c_5	0	h_6	$4A^2+6(Z^P)^2+8AZ^P$
h_3	0	h_7	$-14(Z^P)^2$

the vector-vector-pseudoscalar three-point correlation functions in the three flavor chiral limit (we take the definition given by Eqs. (3) and (4) of [45]). At $p^2=q^2=0$, the loop contributions vanish, and one has (notice the absence of the pion pole in the second equality)

$$\Pi_{VVP}(0,0,r^2)=\frac{2B_0N_c}{16\pi^2r^2}+\frac{1}{4\pi^2}[8A_4-16B_0(A_2-2A_3)],$$

$$\Pi^0_{VVP}(0,0,r^2)=\frac{1}{4\pi^2}[8A_4+24A_6]. \tag{B1}$$

In the chiral limit, the counterterms from $\mathcal{L}^-_{(4,2)}$ do not contribute, so that the above result holds both in SChPT and in GChPT. Although the contributions from the low-energy constants A_2 and A_3 from $\mathcal{L}^-_{6,0}$ were omitted in [45], one may follow the same steps as described there (we have also kept the same notation), and end up with the following set of sum rules:

$$\frac{1}{4\pi^2}[8A_4-16B_0(A_2-2A_3)]=-\frac{B_0}{2M_V^2}\left\{\frac{F_0^2}{M_V^2}+\frac{N_c}{4\pi^2}\left(\frac{M_V}{M_P}\right)^2\tan\Theta\,\frac{\mathcal{A}(\pi'\to\gamma\gamma)}{\mathcal{A}(\pi\to\gamma\gamma)}\right\}, \tag{B2}$$

and

$$\frac{1}{4\pi^2}[24A_6+16B_0(A_2-2A_3)]=-\frac{3}{8}\,\frac{B_0G_{\eta'}}{M^2_{\eta'}}\sqrt{6}\mathcal{A}(\eta'\to\gamma\gamma). \tag{B3}$$

In addition, one needs to know the expression of the amplitude of the two-photon decay of the η, $\mathcal{A}(\eta\to\gamma\gamma)=-t_1(k,\epsilon,k',\epsilon')\mathcal{A}^{\eta\to\gamma\gamma}$, which, in analogy to the $\pi^0\to\gamma\gamma$ amplitude $\mathcal{A}^{\pi^0\to\gamma\gamma}$ of Eq. (4.3), may be written as

$$\mathcal{A}^{\eta\to\gamma\gamma}=\frac{e^2}{4\sqrt{3}\pi^2F_\pi}\left[\frac{F_\pi}{F_\eta}+\frac{1}{3}\hat{m}(5-2r)t+\frac{128}{3}\hat{m}(1-r)A_6+M_\eta^2t'+\hat{m}^2\tilde{t}''(r)+\frac{2}{3}\hat{m}^2(1+2r^2)a_3\right]. \tag{B4}$$

In this last expression, t and t' are related to A_2, A_3, and A_4 according to Eq. (4.9), while r stands for the quark mass ratio $m_s/\hat{m}$, and $\hat{m}^2\tilde{t}''(r)$ denotes the corrections coming from $\mathcal{L}^-_{(4,2)}$, which can be of the orders $\mathcal{O}(\hat{m}^2)$, $\mathcal{O}(\hat{m}m_s)$, and $\mathcal{O}(m_s^2)$.

In the standard case, the two last terms in Eq. (B4) would appear only at higher orders, and one may thus proceed as described in Ref. [45]. At the order we are working, the quark mass ratio is then given as $r_{\rm st}=r_2\equiv 2M_K^2/M_\pi^2-1\sim 25.9$ [16]. Using the numerical values given in [45], one obtains, from Eqs. (B2) and (B3), respectively,

$$\hat{m}A_{4,\rm st}-M_\pi^2(A_2-2A_3)_{\rm st}=(-5.9\pm 1.8)\times 10^{-4} \tag{B5}$$

and

$$3\hat{m}A_{6,\rm st}+M_\pi^2(A_2-2A_3)_{\rm st}=(-2.1\pm 0.4)\times 10^{-3}. \tag{B6}$$

Upon using the experimental rate for $\eta\to\gamma\gamma$ [5], we then determine the combination

$$M_\pi^2(A_2-2A_3)_{\rm st}=(1\pm 1)\times 10^{-3}. \tag{B7}$$

Adding errors in quadrature, the previous results give

$$\hat{m}t_{\rm st}+M_\pi^2t'_{\rm st}=(1.7\pm 8.2)\times 10^{-3}, \tag{B8}$$

which is four times more accurate than the value obtained directly from the experimental rate of $\pi^0\to\gamma\gamma$. For the separate pieces, we obtain

$$\hat{m}t_{\rm st}=(4.4\pm 10.8)\times 10^{-3},\quad M_\pi^2t'_{\rm st}=(-2.7\pm 2.7)\times 10^{-3}. \tag{B9}$$

In the generalized case, the analysis may, unfortunately, not be pursued quite that far. The main drawback are the corrections from $\mathcal{L}^-_{(4,2)}$, which in particular produce potentially large $\mathcal{O}(m_s^2)$ corrections to the $\eta\to\gamma\gamma$ decay amplitude, and on which the sum-rules (B2) and (B3) give no information. If one restricts the analysis to the order $\mathcal{O}(p^5)$ precision, then the contributions from $\mathcal{L}^-_{(6,0)}$ are also absent, and the situation becomes even simpler than in the standard case, since [cf. Eq. (1.4)] the left-hand sides of the sum-rules (B2) and (B3) now only involve A_4 and A_6, respectively. Keeping in mind that r is now a free parameter (α and r are however related, see [17]), and taking the necessary inputs from [45], the $\mathcal{O}(p^5)$ determination of A_4 and A_6 reads

$$\hat{m}A_4=-\frac{N_c}{32}\left(\frac{|\lambda(r)M_S^2-(1-\lambda(r))^2M_\pi^2|}{M_P^2-M_S^2}\right)^{1/2}\frac{M_\pi}{M_P}\,\frac{\mathcal{A}(\pi'\to\gamma\gamma)}{\mathcal{A}(\pi\to\gamma\gamma)}+\cdots, \tag{B10}$$

$$\hat{m}A_6=-\frac{3\pi^2}{32}\,\frac{M_\pi}{M_{\eta'}}\left(\lambda(r)-\frac{\Delta_{\rm GMO}}{(r-1)^2}\right)^{1/2}F_\pi\mathcal{A}(\eta'\to\gamma\gamma)+\cdots, \tag{B11}$$

where the ellipses stand for higher order corrections, $\lambda(r)=2(r_2-r)/(r^2-1)$ and $\Delta_{\rm GMO}\equiv(3M_\eta^2-4M_K^2+M_\pi^2)/M_\pi^2\sim -3.6$. For $r=r_2$, the above expressions give values compatible with the previous SChPT analysis. Furthermore, as r decreases (i.e., as α increases), the variation of $\hat{m}t$ stays within the bounds given in Eq. (B9). On the other hand, in the extreme case of a vanishing condensate, the $\mathcal{L}^-_{(6,0)}$ contributions to the two sum rules also disappear, and the expressions (B10) and (B11) become exact at order $\mathcal{O}(p^6)$. Finally, if we use the two sum rules in order to express A_4 and A_6 in terms of A_2-2A_3 in the expression (B4), we obtain an estimate of a combination of A_2-A_3, $\hat{m}^2\tilde{t}''(r)$ and $\hat{m}^2a_3$, which is not very sensitive to the value of r and compatible with the value (B7) obtained in the standard case for $M_\pi^2(A_2-2A_3)$. Thus, within reasonable error bars, the values of t and t' can be taken independent of r. For the numerical analyses presented in the text, we have used

$$\hat{m}t=(6\pm 12)\times 10^{-3},\quad M_\pi^2t'=(-3\pm 3)\times 10^{-3}. \tag{B12}$$

[1] C. Vafa and E. Witten, Nucl. Phys. **B234**, 173 (1984).

[2] G. 't Hooft, in *Recent Developments in Gauge Theories*, edited by G. 't Hooft *et al.* (Plenum, New York, 1980); Y. Frishman, A. Schwimmer, T. Banks, and S. Yankielowicz, Nucl. Phys. **B177**, 117 (1981); S. Coleman and B. Grossman, *ibid.* **B203**, 205 (1982).

[3] J. Preskill and S. Weinberg, Phys. Rev. D **24**, 1059 (1981).

[4] M. Gell-Mann, R. J. Oakes, and B. Renner, Phys. Rev. **175**, 2195 (1968); S. Glashow and S. Weinberg, Phys. Rev. Lett. **20**, 224 (1968).

[5] Particle Data Group, G. Caso *et al.*, Eur. Phys. J. C **3**, 1 (1998).

[6] J. Stern, ''Two alternatives of spontaneous chiral symmetry breaking in QCD,'' Report No. IPNO-TH-97-41, hep-ph/9801282; contribution to the 205. WE-Heraeus Seminar, Bad Honnef, Germany, 1998, edited by J. Bijnens and U.-G. Meissner, hep-ph/9901381.

[7] J. Stern, in *Chiral Dynamics: Theory and Experiment*, edited by A. M. Bernstein, D. Drechsel, and T. Walcher, Lecture Notes in Physics 513 (Springer-Verlag, Berlin, 1998).

[8] I. I. Kogan, A. Kovner, and M. Shifman, Phys. Rev. D **59**, 016001 (1999).

[9] J. Comellas, J. I. Latorre, and J. Taron, Phys. Lett. B **360**, 109 (1995).

[10] C. Arvanitis, F. Geniet, J. L. Kneur, and A. Neveu, Phys. Lett. B **390**, 385 (1997); J. L. Kneur, Phys. Rev. D **57**, 2785 (1998).

[11] N. H. Fuchs, H. Sazdjian, and J. Stern, Phys. Lett. B **269**, 183 (1991); J. Stern, H. Sazdjian, and N. H. Fuchs, Phys. Rev. D **47**, 3814 (1993); M. Knecht, B. Moussallam, and J. Stern, The π-π Amplitude in Generalized Chiral perturbation Theory, in The Second Daϕne Physics Handbook, edited by L. Maiani, G. Pancheri, and N. Paver, 1995; J. Stern, Nucl. Phys. B (Proc. Suppl.) **B39**, 253 (1995).

[12] M. Knecht, B. Moussallam, J. Stern, and N. H. Fuchs, Nucl. Phys. **B457**, 513 (1995).

[13] G. Ecker, Prog. Part. Nucl. Phys. **35**, 1 (1995); J. Stern, in Proceedings of the *Workshop on Physics and Detectors for DaΦne '95*, edited by R. Baldini, F. Bossi, G. Capon, and G. Pancheri, Frascati Physics Series Vol. IV (INFN-LNF SIS-Ufficio Pubblicazioni, 1995), hep-ph/9510318; M. R. Pennington, in *DAPHCE Workshop on Hadron Dynamics with the New DaΦne and TJNAF Facilities*, Frascati, Italy, 1996 [Nucl. Phys. **A623**, 189c (1997); H. Leutwyler, *ibid.* **A623**, 169c (1997).

[14] S. Weinberg, Physica A **96**, 327 (1979).

[15] J. Gasser and H. Leutwyler, Ann. Phys. (N.Y.) **158**, 142 (1984).

[16] J. Gasser and H. Leutwyler, Nucl. Phys. **B250**, 465 (1985).

[17] M. Knecht and J. Stern, in Generalized Chiral Perturbation Theory, in The Second Daϕne Physics Handbook [11]; M. Knecht, Nucl. Phys. B (Proc. Suppl.) **B39**, 249 (1995).

[18] S. Weinberg, Phys. Rev. Lett. **17**, 616 (1967).

[19] L. Rosselet *et al.*, Phys. Rev. D **15**, 574 (1977).

[20] See, for instance, the contribution of J. Lowe in *Chiral Dynamics: Theory and Experiment* [7], p. 375.

[21] J. Lee-Franzini, in Status of Daphne and KLOE, The Second Daϕne Physics Handbook [11].

[22] B. Adeva *et al.*, proposal to the SpSLC, CERN/SPSLC 95-1, SPSLC/P 284.

[23] S. Adler, B. W. Lee, S. B. Treiman, and A. Zee, Phys. Rev. D **4**, 3497 (1971).

[24] J. W. Bos, Y. C. Lin, and H. H. Shih, Phys. Lett. B **337**, 152 (1994).

[25] P. Talavera, Ll. Ametller, J. Bijnens, A. Bramon, and F. Cornet, Phys. Lett. B **376**, 186 (1996).

[26] P. Talavera, Ph.D. dissertation, Universitat de Barcelona, 1997 (unpublished).

[27] H. W. Fearing and S. Scherer, Phys. Rev. D **53**, 315 (1996).

[28] J. Bijnens, G. Colangelo, and G. Ecker, J. High Energy Phys. **9902**, 020 (1999).

[29] J. Bijnens, Int. J. Mod. Phys. A **8**, 3045 (1993).

[30] D. Issler, Report No. SLAC-PUB-4943 (1989; revised 1990).

[31] R. Akhoury and A. Alfakih, Ann. Phys. (N.Y.) **210**, 81 (1991).

[32] J. F. Donoghue and D. Wyler, Nucl. Phys. **B316**, 289 (1989).

[33] J. Bijnens, A. Bramon, and F. Cornet, Z. Phys. C **46**, 599 (1990).

[34] G. Chew and S. Mandelstam, Phys. Rev. **119**, 467 (1960).

[35] C. Riggenbach, J. Gasser, and J. F. Donoghue, Phys. Rev. D **43**, 127 (1991); J. Bijnens, G. Colangelo, and J. Gasser, Nucl. Phys. **B427**, 427 (1994).

[36] M. R. Pennington and J. Portolés, Phys. Lett. B **334**, 399 (1995); D. Toublan, Phys. Rev. D **53**, 6602 (1996); B. Ananthanarayan and P. Büttiker, *ibid.* **54**, 5501 (1996); G. Wanders, *ibid.* **56**, 4328 (1997).

[37] J. Bijnens, G. Colangelo, G. Ecker, J. Gasser, and M. E. Sainio, Phys. Lett. B **374**, 210 (1996); Nucl. Phys. **B508**, 263 (1997).

[38] L. Girlanda, M. Knecht, B. Moussallam, and J. Stern, Phys. Lett. B **409**, 461 (1997).

[39] J. Gasser, in The $\pi\pi$ Scattering Amplitude in Chiral Perturbation Theory, The Second Daϕne Physics Handbook [11].

[40] M. Knecht, B. Moussallam, J. Stern, and N. H. Fuchs, Nucl. Phys. **B471**, 445 (1996).

[41] L. Girlanda and J. Stern, Report No. IPNO-TH/99-09, hep-ph/9906489; L. Girlanda (in preparation).

[42] D. Morgan and G. Shaw, Nucl. Phys. **B10**, 1387 (1969).

[43] J. Bijnens, G. Colangelo, and P. Talavera, J. High Energy Phys. **05**, 014 (1998).

[44] A. Manohar and H. Georgi, Nucl. Phys. **B234**, 189 (1984); H. Georgi and L. Randall, *ibid.* **B276**, 241 (1986); H. Georgi, Phys. Lett. B **298**, 187 (1993).

[45] B. Moussallam, Phys. Rev. D **51**, 4939 (1995).

[46] Proceedings of the *Third Workshop on the Tau–Charm Factory, Marbella (Spain), 1–6 June 1993*, edited by J. Kirkby and R. Kirkby (Editions Frontières, Gif-sur-Yvette, France, 1994); M.L. Perl and C. Kim, Report No. SLAC-PUB-8094 (1999).

[47] A. Courau and G. Pancheri, in The Daϕne Physics Handbook, edited by L. Maiani, G. Pancheri, and N. Paver, 1992.